

Dynamic control of adipose tissue development and adult tissue homeostasis by platelet-derived growth factor receptor alpha

Sunhye Shin^{1*}, Yiyu Pang^{1*}, Jooman Park¹, Lifeng Liu¹, Brandon E Lukas¹, Seung Hyeon Kim², Ki-Wook Kim², Pingwen Xu³, Daniel C Berry⁴, and Yuwei Jiang^{1,5}

¹Department of Physiology and Biophysics, College of Medicine, The University of Illinois at Chicago, Illinois, 60612, USA

²Department of Pharmacology, College of Medicine, The University of Illinois at Chicago, Chicago, Illinois, 60612, USA

³Division of Endocrinology, Department of Medicine, The University of Illinois at Chicago, Chicago, Illinois, 60612, USA

⁴Division of Nutritional Sciences, Cornell University, Ithaca, NY 14853

*Co-first author

⁵Corresponding author

Email addresses:

yuweij@uic.edu

Telephone and fax numbers of the corresponding author:

Phone: +1-312-413-7261

Fax: +1-312-996-1414

Abstract

Adipocytes arise from distinct progenitor populations during development and adult, but little is known about how developmental progenitors differ from adult progenitors. Here, we investigate the role of platelet-derived growth factor receptor alpha (PDGFR α) in the divergent regulation of the two different adipose progenitor cells (APCs). Using *in vivo* adipose lineage tracking and deletion mouse models, we found that developmental PDGFR α ⁺ cells are adipogenic and differentiated into mature adipocytes, and the deletion of *Pdgfra* in developmental adipose lineage disrupted white adipose tissue (WAT) formation. Interestingly, adult PDGFR α ⁺ cells do not significantly contribute to adult adipogenesis, and deleting *Pdgfra* in adult adipose lineage did not affect WAT homeostasis. Mechanistically, embryonic APCs require PDGFR α for fate maintenance, and without PDGFR α , they underwent fate change from adipogenic to fibrotic lineage. Collectively, our findings indicate that PDGFR α ⁺ cells and *Pdgfra* gene itself are differentially required for WAT development and adult WAT homeostasis.

Keywords: PDGFR α ; Adipose progenitor cells; Adipose tissue development; Adipose tissue homeostasis; adipogenesis

1. Introduction

White adipose tissue (WAT) is a dynamic endocrine organ that controls important physiological processes and mediates various metabolic responses (Kershaw and Flier, 2004; Rosen and Spiegelman, 2006, 2014; Spiegelman and Flier, 2001; Trayhurn and Beattie, 2001). However, the development of WAT is not well understood. Adipocytes are constantly replenished with new adipocytes derived from the stem cell pool, a process named adipogenesis (Cawthorn et al., 2012; Sebo and Rodeheffer, 2019). In young adult mice, the rate of adipogenesis has been estimated at 10%–15% per month (Rigamonti et al., 2011), and retrospective human studies also indicate a high turnover rate (Spalding et al., 2008). Under homeostatic conditions, the process is relatively constant, but it is sensitive to pharmacologic, physiologic, and dietary stimuli. For instance, adipose tissues can expand from 2%–3% to 60%–70% of body weight in response to a positive energy balance through both hyperplasia and hypertrophy (Ginsberg-Fellner, 1981; Hirsch and Batchelor, 1976; Hirsch and Knittle, 1970; Jo et al., 2009; Knittle et al., 1979). Notably, the thiazolidinedione (TZD) class of diabetes treatments increase *de novo* adipogenesis by stimulating stem cell compartment self-renew and proliferation (Tang et al., 2011). Both childhood and adult obesity are caused by uncontrolled expansion of WAT and excessive lipid accumulation, which elevate the risk of metabolic disorders (Berry et al., 2016a; Hajer et al., 2008; Jiang et al., 2012b; Smorlesi et al., 2012). However, the underlying differences between these two types of obesity are not clear yet. Therefore, there is a clear clinical need to investigate how WAT is developed, maintained and expanded during developmental and adult stages.

Recently, multiple genetic fate-mapping and lineage-marking studies have been conducted to understand when and where adipose progenitor cells (APCs), which are capable to proliferate and differentiate into new adipocytes, are specified (Cattaneo et al., 2020; Jiang et al., 2014; Lee et al., 2013a; Lee et al., 2013b; Sanchez-Gurmaches and Guertin, 2014; Sanchez-Gurmaches et al., 2015; Sebo et al., 2018; Tang et al., 2008; Tran et al., 2012;

Vishvanath et al., 2015; Wang et al., 2013). For example, it was reported that adult adipocytes, but not developmental adipocytes, are differentiated from a perivascular smooth muscle actin (SMA, encoded by *Acta2* gene) mural cell source to reside along the blood vessel walls within WAT (Jiang et al., 2014). The following study identified that platelet-derived growth factor receptor beta (PDGFR β) mediates the interaction and communication between adult SMA+ APC and niche (Jiang et al., 2017b). Lineage tracing studies reveal that adipose mural PDGFR β + cells do not contribute to adult homeostasis but contribute to adipose remodeling in obese or cold exposed adult mice (Vishvanath et al., 2016). These findings reveal that adipocytes arise from diverse lineages and that there are at least two different adipose progenitor populations, including developmental progenitors used for adipose tissue organogenesis and adult progenitors used for adipose tissue homeostasis. However, the origin and identity of the developmental progenitors remain to be determined. Also, it is not clear whether developmental and adult progenitors utilize different regulatory mechanisms to give rise to functionally different adipocytes. Recent studies suggest that, even within a single adipose depot, there appears to be multiple subpopulations of adipocytes (Lee et al., 2019).

Platelet-derived growth factor receptor alpha (PDGFR α) is a membrane-bound tyrosine kinase receptor expressed in perivascular stromal cells within a variety of tissues. PDGFR α has been commonly used as a cell surface marker for adipose progenitor identification, and multiple studies have reported that PDGFR α + cells generate adipocytes in response to adipogenic stimuli (Berry and Rodeheffer, 2013; Cattaneo et al., 2020; Joe et al., 2010; Lee et al., 2012a; Lee et al., 2012b; Rivera-Gonzalez et al., 2016). For example, using *Pdgfra*^{Cre}; *Rosa26R*^{mT/mG} mice, PDGFR α marks adipocytes (Berry and Rodeheffer, 2013). Also, WAT-resident PDGFR α + cells can develop into brown-like adipocytes in response to β 3-adrenergic agonist or white adipocytes in response to high-fat diet feeding (Lee et al., 2012b). Recent studies have shown that there are two subsets of PDGFR α + cells in adipose tissues delineated by CD9 expression. Whereas CD9-high PDGFR α + cells are pro-fibrogenic and drive adipose tissue fibrosis, CD9-

low PDGFR α ⁺ cells are pro-adipogenic and make adipocytes (Marcelin et al., 2017). In addition, increased PDGFR α activity drives adipose tissue fibrosis during both adult homeostasis and adipose tissue organogenesis (Iwayama et al., 2015; Sun et al., 2017). However, due to the complexity and nonspecificity of the mouse lines, our understanding of the role of PDGFR α ⁺ cells *in vivo* has been limited. Further clarification of PDGFR α ⁺ cell fate by lineage tracing studies at different time points is still needed. In addition, loss-of-function models generated in developmental or adult adipose lineage are required to definitively determine the physiological functions of PDGFR α in different stages.

In the present study, we aim to understand the role of PDGFR α ⁺ cells and the gene itself in different stages of adipose tissue (postnatal development and adult maintenance of WAT) using *in vivo* adipose lineage tracking and gene deletion systems. We found that PDGFR α ⁺ cells are a progenitor source for postnatal WAT development but not adult WAT homeostasis. Consistently, *Pdgfra* expression in APCs is not essential for adult WAT homeostasis but required for postnatal WAT development. Deletion of *Pdgfra* in adult APCs did not disrupt adult WAT maintenance and cold-induced beige adipocyte formation. However, deletion of *Pdgfra* in developmental APCs led to significant fat reduction associated with smaller fat depots. Mechanistically, embryonic PDGFR α -deficient APCs were unable to differentiate into mature adipocytes and underwent fate change from adipogenic to fibrotic lineage. Together, our findings unraveled a dynamic requirement for PDGFR α ⁺ cells and *Pdgfra* gene itself in controlling WAT development and WAT homeostasis.

2. Results

2.1. Developmental adipocytes derive from a PDGFR α ⁺ cell source

Our previous work demonstrated that adult but not developmental adipocytes emanate from a vascular smooth cell expressing smooth muscle actin (SMA) and other mural markers (Jiang et al., 2017b; Jiang et al., 2014). However, the specific origins for developmental APCs remain

unknown. We proposed to test the possibility of using PDGFR α as a fate marker for the developmental APCs. PDGFR α is a membrane-bound tyrosine kinase receptor that has been used as a cell surface marker for adipose progenitor identification. Moreover, multiple studies using several *Pdgfra* genetic tools have shown that PDGFR α + cells can mark the adipose lineage and generate adipocytes (Berry and Rodeheffer, 2013; Lee et al., 2012b). We hypothesized that PDGFR α + cells mark the developmental APCs, but not adult APCs, and contribute to adipose tissue organogenesis and development.

To investigate the fate mapping of PDGFR α + cells, we marked and monitored PDGFR α + cells using *Pdgfra*^{Cre-ERT2}; *Rosa26R*^{RFP} (PDGFR α -RFP) mice. Using this model, we previously reported *Pdgfra*^{Cre-ERT2} dependent RFP reporter expression faithfully labels adipose tissue resident PDGFR α + cells and their descendants (Berry et al., 2016b; Lee et al., 2012b). To avoid potential off-target effects of tamoxifen (Ye et al., 2015) and to induce *Pdgfra*-dependent recombination, we provided one dose of tamoxifen at P10 (adipose tissue organogenesis) or P60 (established depots for adipocyte turnover and maintenance), and examined reporter expression at pulse (P13 or P63; pulse) or after a 2-month chase (P60 or P120). Both whole mount and immunohistochemistry (IHC) studies indicated that, at pulse (P13 or P63), PDGFR α -dependent RFP expression was restricted to the perivascularity in subcutaneous inguinal WAT (IGW), perigonadal WAT (PGW), and brown adipose tissue (BAT). As expected, mature adipocytes were not labeled as previously reported (Berry et al., 2016b; Berry and Rodeheffer, 2013; Lee et al., 2012b) (**Figure 1_Figure supplement 1**). However, P10 to P60 chase revealed the elaboration of RFP expression into adipocytes in both male and female IGW and BAT, but not in PGW suggesting the creation of new adipocytes from a PDGFR α + source (**Figure 1A**). Of note, there was strong RFP+ labeling in the male epididymis (**Figure 1A**). Surprisingly, during the P60 to P120 chase, we observed minimal RFP-adipocyte labeling in IGW, PGW, and BAT (connected with interscapular WAT) based on whole-mount

images (**Figure 1B**). Interestingly, we did not observe fate mapping difference between male and female adipose depots (**Figure 1A,B**).

To further deduce the contribution of PDGFR α + lineage during WAT development and maintenance, we quantified RFP+ cells in adipose tissue sections from PDGFR α -RFP mice (RFP marks PDGFR α + lineage and their descendants) injected with tamoxifen at P10 or P60 and perfused at P60 or P120. Consistent with the results from whole mount imaging, there were RFP+ adipocytes in IGW and BAT depots but not PGW depots from P10-P60 chow-fed male mice (IGW 20-30%; PGW 0%; BAT 30-35%) (**Figure 1C**). In contrast to developmental labeling, we observed significantly less RFP+ (roughly 2%) adipocyte labeling of WAT and BAT depots from male mice. Rather our IHC studies demonstrated the presence of PDGFR α -RFP+ cells residing in perivascular positions, similar to pulse (**Figure 1D**). In a separate study, PDGFR α -reporter mice were administered tamoxifen at P60 and chased to P180. Again, we observed very few adipocytes labeled by PDGFR α -RFP+ cells rather these cells appeared to be restricted to the vasculature of both WAT and BAT (**Figure 1_Figure supplement 1**). Together, it appears, under our conditions, that PDGFR α + cells give rise to developmental adipocytes, but not a major APCs for adult adipocytes.

2.2. Developmental, but not adult, PDGFR α + cells are a cellular origin of adipogenesis associated with high-fat diet and TZD feeding

It has been reported that PDGFR α + cells contribute to adipose tissue expansion in response to high-fat diet (HFD) (Lee et al., 2012b). To test if the fate mapping potential of PDGFR α -RFP+ cells change in response to HFD challenge, we fed Tamoxifen-induced PDGFR α -RFP reporter mice from P10-P60 or P60-P120 with chow diet or HFD (60% of calories from fat). To our surprise but in agreement with our fate mapping studies above, we found very few PDGFR α -RFP+ generated adipocytes during the P60-120 HFD challenge (**Figure 1B,D**). In contrast, developmental HFD fate mapping demonstrated a strong correspondence between RFP

reporter expression and adipocytes labeling in IGW and BAT but not PGW. Quantification indicated that ~90% of IGW and ~95% of brown adipocytes were RFP+ whereas only ~5% PGW adipocytes were labeled (**Figure 1A,C; Figure 1_Figure supplement 1**). The low labeling of PGW could reflect the developmental specification of this depot, as this depot has been shown to be specified beyond P10. Together, our fate-mapping data suggest that P10 but not P60 labeled PDGFR α + stromal vascular (SV) cells are adipogenic. HFD-fed mice utilize only the developmental but not adult labeled PDGFR α + cells as a cellular source for adipose tissue expansion.

Peroxisome proliferator activated receptor gamma (PPAR γ) is a master regulator of adipogenesis (Farmer, 2006; Lehrke and Lazar, 2005). PPAR γ agonists such as rosiglitazone (Rosi), a thiazolidinedione (TZD), have been reported to trigger the formation of new adipocytes from an adult adipose stem/progenitor compartment (Crossno et al., 2006; Tang et al., 2011). To test whether adult PDGFR α + cells can acquire adipogenic potential when exposed to PPAR γ agonists, we administered Rosi to PDGFR α -RFP+ mice for 8 weeks (**Figure 1_Figure supplement 1**). We observed that the PDGFR α -dependent RFP expression remained restricted at the vasculature, and there were rare RFP+ labeled adipocytes, based upon lipidTox and perilipin staining of IGW sections (**Figure 1_Figure supplement 1**). These data suggest that in response to TZDs administration, PDGFR α + cells may not represent a major progenitor cell population for new adipocytes.

2.3. Developmental and adult PDGFR α + cells have distinct molecular and functional signatures

To examine the *in vitro* adipogenic potential of P10 and P60 PDGFR α + cells, we isolated total SV cells from IGW from tamoxifen-pulsed PDGFR α -RFP mice (P13 or P63; pulse). This fraction contains both RFP+ and RFP negative (RFP-) cells. Cells were cultured for seven-days in white adipogenic conditions. Consistent with our fate-mapping data, the SV cells from P13 mice

196 produced RFP labeled mature adipocytes (>75% of total adipocytes are RFP+) (**Figure 2A**). In
197 contrast, the SV cell cultures from P63 PDGFR α -RFP mice generate very few RFP+ adipocytes
198 (<5% of total adipocytes are RFP+) and PDGFR α -RFP+ cells retained their fibroblast
199 morphology (**Figure 2B**). Using fluorescence-activated cell sorting (FACS), we isolated P10
200 tamoxifen-pulsed PDGFR α -RFP SV cells into RFP+ and RFP- cells and subsequently cultured
201 them in adipogenic media for seven-days. Cultures containing FACS-isolated P10 RFP+ had
202 many RFP+ adipocytes and were overall more adipogenic compared to P10 RFP- cells as
203 assessed by lipid content and adipocyte gene expression (**Figure 2C,D**). These data are
204 consistent with our *in vivo* lineage-tracing data, indicating that developmental PDGFR α + cells
205 are adipogenic.

206 Our *in vivo* lineage-tracing data and *in vitro* primary cell culture data indicated that WAT
207 organogenesis requires PDGFR α + cells while adult WAT homeostasis utilized a different APC
208 source. We next investigated whether the molecular basis of P10 and P60 PDGFR α + cells were
209 distinct. We FACS-sorted P10 and P60 tamoxifen-pulsed PDGFR α -RFP SV cells into RFP+ and
210 RFP- cells (**Figure 2E**). FACS-isolated P10 PDGFR α + cells had a significantly higher levels of
211 pre-adipogenic markers (*Pparg*, *Pref1*, *Zfp423*) compared to P60 PDGFR α + cells (**Figure 2E**).
212 In contrast, levels of fibroblast markers (*Col1a1* and *Col3a1*) and *Cd24* (a proposed APC
213 marker) displayed no significant difference between P10 and P60 PDGFR α + cells (**Figure 2E**).
214 We also did not observe any differences in the expression of mature adipocyte markers
215 (*Fabp4*, *Plin1*, *Adipoq*) and endothelial markers (*Cd31*, *VE-cadherin*) (**data not shown**).

216 To further assess PDGFR α 's contribution to the APC lineage, we combined the
217 PDGFR α -RFP reporter mouse model with the doxycycline suppressible adipose lineage track
218 system, AdipoTrak (*Pparg*^{TA}; TRE-Cre; TRE-*H2B-GFP*) (Jiang et al., 2017b; Tang et al., 2008).
219 AdipoTrak labeled cells have been shown to be necessary for WAT formation and adipocytes
220 homeostasis and marks the entire adipose lineage (stem-to-adipocyte) (Jiang et al., 2017b;
221 Tang et al., 2008). This dual model will allow for spatiotemporal lineage identification and

overlap between PDGFR α -RFP+ cells and AdipoTrak-GFP+ cells (**Figure 2_Figure supplement 1**). Dual reporter mice were tamoxifen-induced at P10 or P60 and SV cells from WATs were isolated three-days later. Flow cytometric quantification, using RFP as a surrogate for PDGFR α and GFP for PPAR γ , identified strong correspondence between RFP and GFP in P10 samples (IGW 15.36%; PGW 8.25%; BAT 6.63%), but not at P60 (**Figure 2F; Figure 2_Figure supplement 1**). Together, these results indicate that P10 but not P60 PDGFR α + cells express adipose progenitor markers, which might account for their differences in adipogenic capabilities.

2.4. Developmental PDGFR α + cells contribute to postnatal but not adult WAT development

To test whether these P10 labeled PDGFR α -RFP+ cells still maintain adipogenic potential in the adult stage, we performed fate mapping tests from P10-P120. WAT whole-mount imaging showed that PDGFR α + SV cells labeled at P10 made adipocytes which could still be observed at P120 in IGW under both chow- and HFD-fed conditions (**Figure 3A; Figure 3_Figure supplement 1**). We quantified the number of PDGFR α -RFP+ adipocytes between P10-P120 fate mapping with our P10-P60 fate mapping studies. Interestingly, we found that the percentage of RFP+ adipocyte labeling from P10-P120 was either maintained or significantly reduced compared to RFP- adipocyte labeling from P10-P60 (Chow P10-P120: IGW ~20%; PGW ~20%; BAT ~5%, HFD P10-P120: IGW ~5%; PGW ~10%; BAT ~10%) (**Figure 3_Figure supplement 1**). Thus, our fate mapping data suggest that postnatal P10 PDGFR α + cells do not continue to contribute to adult WAT homeostasis or HFD-induced expansion.

To validate the notion that adult PDGFR α + cells do not contribute to adult WAT homeostasis, we revisited constitutive *Pdgfra*^{Cre} mouse model and combined it with *Rosa26R*^{RFP} reporter. Lineage marking analysis demonstrated different labeling results in IGW depots at two-month-old and six-month-old. We found nearly all IGW mature adipocytes (95-100%), at two-

month-old, were labeled with RFP. Yet, at six-month, we found minimal RFP-adipocyte marking (10-15%) (**Figure 3B**). These data suggest that adipocytes generated in the adult homeostatic phase were derived from a PDGFR α -independent source. To further confirm this, we generated a deletion model, in which PPAR γ , the master regulator of adipogenesis, was constitutively deleted in PDGFR α + cells, to block adipocyte differentiation. We observed that there was a severe disruption of IGW development at 2-month-old mice, revealing the importance of PDGFR α + cells for adipose tissue development. However, 6-month-old mice showed recovered IGW tissue size with normal adipocytes number (**Figure 3C**). These data support the possibility that developmental PDGFR α + cells are used for WAT development, but adult WAT maintenance does not utilize PDGFR α + cells as a progenitor source.

To further evaluate the necessity of the PDGFR α + cells in a cell-autonomous manner, we combined the *Pparg*^{f/f} conditional mouse model with the tamoxifen-inducible *Pdgfra*^{Cre-ERT2}. This model will provide spatiotemporal deletion of *Pparg* to test the necessity of PDGFR α + cells to generate new white adipocytes. At P60, we isolated SV cells from un-induced *Pdgfra*^{Cre-ERT2}; *Pparg*^{f/f} (PDGFR α -PPAR γ -KO) mice. We then cultured the cells in adipogenic media containing either vehicle or 4-OH-tamoxifen (2 μ M/mL). Consistent with the *in vivo* lineage tracing data, SV cells from control and PDGFR α -PPAR γ -KO mice that received 4-OH-tamoxifen underwent adipogenesis similarly as indicated by Oil Red O staining and adipocyte marker expression (**Figure 3_Figure supplement 1**). These results support the notion that adult labeled PDGFR α + cells are not an essential cellular source for adipogenesis.

2.5. PDGFR α in adult SMA+ APCs is not required for adult white or beige adipogenesis under physiological conditions

Our *in vivo* and *in vitro* data show that PDGFR α + cells do not contribute to adult WAT homeostasis. SMA+ cells were reported as adult adipose progenitor cells required for adult WAT homeostasis and turnover (Jiang et al., 2014). Further, this study showed that some

274 SMA+ cells express PDGFR α . Flow analysis indicated that about half of the RFP labeled SMA+
275 cells expressed PDGFR α , and this was confirmed by quantitative PCR analysis, showing a ~10
276 fold enrichment of *Pdgfra* mRNA expression in RFP labeled SMA+ cells. Thus, we hypothesized
277 that PDGFR α in SMA+ cells could potentially regulate APC function and differentiation. To test
278 this notion, we combined the *Pdgfra*^{f/f} conditional mouse model with APC lineage tracking and
279 deletion tool, *Acta2*^{Cre-ERT2}; *Rosa26*^{RFP} to create *Acta2*^{Cre-ERT2}; *Pdgfra*^{f/f} (SMA-PDGFR α -KO;
280 **Figure 4A,B**). At P60 mice were administered one dose of tamoxifen for two consecutive days
281 and mice were analyzed 30 days later. Consistent with the PDGFR α fate-mapping studies, at
282 P90, we observed no physiological difference between control and SMA-PDGFR α -KO mutant
283 mice under chow diet feeding. The control and mutant mice had similar body weight (**Figure**
284 **4C**), fat mass (**Figure 4_Figure supplement 1**), food intake (**Figure 4_Figure supplement 1**),
285 adipose tissue weights (**Figure 4D**), and glucose clearance (**Figure 4E**). As expected, SMA-
286 PDGFR α -KO mutant BAT had reduced expression of *Pdgfra* (**Figure 4_Figure supplement 1**).
287 Histologically, we did not observe obvious phenotypic difference between control and mutant
288 WAT or BAT morphology and architecture (**Figure 4F**). We also assessed fate mapping
289 analysis of control and SMA-PDGFR α -KO APCs to produce adipocytes. In line with our previous
290 observations, control APCs generated RFP labeled adipocyte (**Figure 4G**). Similarly, SMA-
291 PDGFR α -KO APCs also generated white adipocytes with the same efficiency (**Figure 4G**).
292 Thus, our fate-mapping data support that new adipocytes generated from SMA+ cells (RFP+) in
293 both IGW and PGW are not affected by *Pdgfra* deletion. To exclude the possibility that SMA-
294 PDGFR α -KO cells generated dysfunctional adipocytes, we examined metabolic performance
295 using metabolic cage analysis of control and mutant mice at P90, after a 30 day chase. We
296 observed that control and mutant mice showed similar energy expenditure, oxygen
297 consumption, carbon dioxide production, and respiratory exchange ratio (**Figure 4_Figure**
298 **supplement 1**). Taken together, these data indicate that PDGFR α does not play a significant
299 role in the ability of adult APCs to generate adipocytes and maintain adult WAT homeostasis.

To further evaluate if PDGFR α functioned in SMA+ APCs, we isolated SV cells from Tamoxifen pulse Control and SMA-PDGFR α -KO mice at P60 and subsequently culture them in adipogenic media. The adipogenic potential of SMA-PDGFR α -KO cells appeared similar to Control SV cells as assessed by Oil Red O staining (**Figure 4H**).

Previous fate-mapping studies using *Acta2*^{Cre-ERT2} revealed that SMA+ WAT resident perivascular cells also serve as beige progenitors: new beige adipocytes are formed in WAT rapidly when mice are exposed to cold, in part through *de novo* differentiation from SMA+ progenitors (Berry et al., 2016b). Therefore, we decided to examine if PDGFR α is required for beige adipogenesis using the SMA-PDGFR α -KO mouse model. We administered one dose of Tamoxifen for two consecutive days to both control and mutant mice at P90 and then waited two weeks prior to cold exposure (6.5°C) (**Figure 5A**). Both control and mutant mice had a similar rectal temperature, a surrogate for beiging, at the end of cold exposure (**Figure 5B**). SMA-PDGFR α -KO mice had similar body weight, serum glucose level and adiposity as controls after cold exposure (**Figure 5C-E**). Histologically, H&E staining and UCP1 IHC of IGW and PGW showed similar results in control and mutant mice (**Figure 5F,G**). There was also no significant BAT morphological difference between control and mutant mice (**Figure 5_Figure supplement 1**). Consistent with H&E staining, qPCR analysis of thermogenic genes (*Ucp1*, *Prdm16*, and *Cidea*) from whole IGW depots suggested no significant difference between control and mutant beige adipocyte potential (**Figure 5_Figure supplement 1**). These data suggest that PDGFR α may not have a functional role in adult SMA+ APCs in altering their ability to generate cold-inducible beige adipocytes.

2.6. PDGFR α in developmental APCs is essential for adipose tissue development

Our data thus far suggests that PDGFR α does not have a functional role in adult adipogenic potential. Therefore, we decided to re-examine PDGFR α 's role in WAT organogenesis and combined the AdipoTrak (AT) adipose lineage tracking and deletion system (*Pparg*^{tTA}; TRE-Cre;

TRE-*H2B-GFP*) (Tang et al., 2008) with the *Pdgfra*^{fl/fl} conditional mouse model (*Pparg*^{tTA}; TRE-*Cre*; TRE-*H2B-GFP*; *Pdgfra*^{fl/fl}=AT-PDGFR α -KO) (**Figure 6A**). Of note, AdipoTrak labeled P10 and P30 cells express *Pdgfra* based on qPCR analysis (Jiang et al., 2014). Although control and AT-PDGFR α -KO mice displayed similar body weight at P60 (**Figure 6B**), AT-PDGFR α -KO mutant mice showed smaller adipose depots and reduced WAT weights (**Figure 6C,D**). In contrast, the weights of other tissues such as liver, kidney, spleen, pancreas, muscle and heart showed no difference compared to controls (**Figure 6E**). Glucose tolerance test showed that mutant mice had impaired glucose tolerance, which may be due to the deficiency of functional adipocytes (**Figure 6F**). Histological staining revealed a paucity in adipocytes and only remnant adipocytes could be observed in mutant IGW and interscapular WAT (ISCW) (**Figure 6G**; **Figure 6_Figure supplement 1**). Lipodystrophy is often accompanied by other metabolic disturbances such as liver steatosis; however, mutant mice did not appear to display fatty liver disease at this stage of life (**Figure 6_Figure supplement 1**). We also evaluated the cell-autonomous adipogenic potential of SV cells. Specifically, SV cell were isolated from control and mutant mice and cultured them in adipogenic media. Compared to control cells which are highly adipogenic, the AT-PDGFR α -KO mutant cells did not display adipogenic potential based upon appearance and Oil Red O staining (**Figure 6H**). These data strongly indicate that PDGFR α in developmental APCs is essential for adipose tissue development.

2.7. PDGFR α regulates adipose tissue development

Our histological staining of AT-PDGFR α -KO WAT demonstrated the lack of adiposity with fibrotic tissue replacement; therefore, we tested if PDGFR α loss leads to fibrosis. Trichrome collagen staining of IGW depots showed presence of fibrotic tissue in mutant but not in control specimens (**Figure 7A**). We then assessed if APCs deficient in PDGFR α resulted in a changes in APC locality and number. Whole-mount imaging of control and mutant WAT demonstrated the presence of GFP+ APCs in the correct anatomic anlage (**Figure 7B**). PDGFR α -deficient

GFP+ cells also appeared to occupy the correct perivascular niche position (**Figure 7_Figure supplement 1**). We then performed FACS analysis on GFP+ APC number, and found AT-PDGFR α -KO mice had many more GFP+ progenitors than control WAT (control: 14.4% of SV cells; mutant: 59.9% of SV cells) (**Figure 7C-D**). Further analysis of these depots via FACS showed an increase in the endothelial marker *Cd31* (PECAM) (**Figure 7C**). Directed qPCR analyses of the FACS-isolated GFP+ cells from the AT-PDGFR α -KO mutant mice verified the reduction in *Pdgfra* mRNA expression. Mutant GFP+ cells had lower expression of adipogenic markers, including *Pparg*, *Fabp4*, *Plin1*, and *Lep* (**Figure 7E**). Consistent with the trichrome collagen staining, mutant GFP+ cells had higher expression of fibroblast markers, such as *Col1a1*, *Col3a1*, *Col6a1*, and *Ddr2*, compared to those from the control mice (**Figure 7F**). These data suggest that the loss of PDGFR α within the APC lineage promotes fibrotic gene expression rather than the adipogenic program. This could be a potential rationale for the fibrotic tissue incorporation in these WATs and could suggest a lineage fate switch (**Figure 7G**).

3. Discussion

APCs are key components for WAT formation, maintenance, and expansion, and a variety of external stimuli can influence adipose homeostasis by controlling the regulatory mechanisms (Berry et al., 2013; Berry et al., 2014; Hepler et al., 2017; Jiang et al., 2012a; Sebo and Rodeheffer, 2019; Tang et al., 2008). Distinct populations of APCs have been identified, but their relationship and the relevance to physiological and pathological adipose expansion remains unknown. We previously reported that there are two distinct adipose progenitor compartments, developmental and adult, which are utilized for adipose organogenesis and adipose homeostasis, respectively (Jiang et al., 2014). We have demonstrated that these two different progenitor pools have different microanatomical, functional, morphological, genetic, and molecular profiles. Notably, adult progenitors fate-map from a SMA+ mural cell lineage while developmental progenitors do not (Jiang et al., 2014). However, the identity of

developmental APCs and the regulatory mechanisms governing WAT development and homeostasis were unclear. In the current study, we attempted to disentangle these two APC populations by using a PDGFR α tamoxifen-inducible lineage-tracing system. We find that PDGFR α + cells generate adipocytes during development but not during adult WAT homeostasis. Further, we show that the role of PDGFR α is differentially required. For example, during development, PDGFR α signaling is important for APCs to generate mature adipocytes. On the other hand, during WAT homeostasis, PDGFR α signaling in SMA+ adult APCs is dispensable for both white and cold-induced beige adipocyte formation. Our results implicate PDGFR α as a regulator of developmental APC lineage specification and adipogenesis in turn promoting WAT organ development.

Our study provides fate-mapping and genetic evidence that PDGFR α is differentially required for adipogenesis at different times of lifespan, revealing the distinct regulatory mechanism governing adipose tissue development versus adult adipose tissue homeostasis *in vivo*. Other studies also suggest the existence of distinct regulatory mechanisms for WAT development and maintenance (Shao et al., 2017; Wang et al., 2015). It is reported that CEBPA (CCAAT Enhancer Binding Protein Alpha), a critical transcription factor expressed during adipogenesis, is not required for WAT development and maintenance during fetal and early postnatal stage, but essential for the obesogenic expansion of WAT induced by HFD (Wang et al., 2015). ZFP423 (zinc finger protein 423), expressed in committed preadipocytes (Gupta et al., 2012), is shown to regulate adipocyte differentiation during fetal adipose development; however, in adult mice, it controls a white-to-beige phenotypic switch (Shao et al., 2017). Also, *Adipoq* driven Cre is more actively expressed at an earlier stage of the adipocyte life cycle during fetal WAT development compared to adult mice (Shao et al., 2017). Jeffery et al. reported that AKT2 (Serine/Threonine Kinase 2) is dispensable for adipose tissue development but required for CD24+ adipose progenitor cell proliferation in postal animals (Jeffery et al., 2015). These studies consistently indicate that developmental and adult APCs utilize distinct

regulatory mechanisms to respond to developmental and nutritional cues. The findings may also hint that adipocytes generated during developmental and adult have distinct functions.

Our data suggest that PDGFR α signaling, specifically in SMA+ APC, does not play a significant role in SMA+ progenitors' differentiation into adipocytes under physiological condition. It is unclear at this point whether PDGFR α signaling in adult APCs has other important functions under pathological conditions. For example, PDGFR α signaling might be essential for the obesogenic expansion and fibrotic response of WAT induced by HFD. This hypothesis, while speculative, is consistent with several studies reported that overexpressing PDGFR α inhibits adipogenesis and promotes fibrosis (Hepler et al., 2017; Iwayama et al., 2015; Lee et al., 2012a; Marcelin et al., 2017; Sun et al., 2017). A more specific study showed that a subset of PDGFR α + cells with high CD9 expression, induced by obesity, originates pro-fibrotic cells, while those with low CD9 expression are committed to adipogenesis (Iwayama et al., 2015; Sun et al., 2017). HFD feeding triggers the recruitment of PDGFR α + cells (Marcelin et al., 2017) and obesity induces CD9 expression in PDGFR α + cells, which become fibrotic cells. Thus, we cannot completely rule out the roles of PDGFR α signaling in adult APCs unless a proadipogenic and a fibrogenic challenge is done in the mice and fibrosis is actually assessed. It will be interesting to challenge SMA-PDGFR α -KO mice with HFD feeding and then test if PDGFR α in adult APCs plays a role in obesogenic WAT expansion.

Several groups have now reported that adipose stromal cells express PDGFR α (Hepler et al., 2017; Iwayama et al., 2015; Lee et al., 2012a; Marcelin et al., 2017; Sun et al., 2017). In addition, fate mapping studies using inducible *Pdgfra-Cre* have been performed in multiple labs. However, the results are strikingly different. For example, a more recent study using *Pdgfra-MerCreMer* lineage traced animals found that PDGFR α + fibroblasts gave rise to brown, beige, and white adipocytes during adult homeostasis (Cattaneo et al., 2020). Another study suggest that PDGFR α + cells are bi-potential to produce both beige and HFD-induced white adipocytes (Lee et al., 2012a). Moreover, another study suggests the balance between PDGFR α /PDGFR β

signaling determines progenitor commitment to beige or white adipogenesis (Gao et al., 2018). Multiple factors may account for this discrepancy. One possible explanation lies in the use of different inducible *Cre* models of *Pdgfra*. The *Pdgfra*-MerCreMer was produced by knocking in the inducible *Cre* cassette into the endogenous *Pdgfra* locus, which represents native *Pdgfra* expression; yet, it may disrupt *Pdgfra* transcription (Ding et al., 2013). In contrast, our *Pdgfra*^{Cre-ERT2} line was generated using BAC transgenic mice (Rivers et al., 2008), which did not affect endogenous expression but may not fully recapitulate the endogenous *Pdgfra* expression. Another potential factor in the difference is the *Cre-loxP* recombination efficiency and cell type specificity. In a previously report (Jiang et al., 2017a), we have characterized the *Pdgfra*^{Cre-ERT2} model and showed that PDGFR α -RFP+ cells were 100% positive for PDGFR α antibody staining, indicating this system can specifically label the cell types of interest, which is PDGFR α +. In the current study, our FACS analysis showed less PDGFR α -RFP labeling at P60 compared to P10 WAT labeling. From our studies, it is unclear why there is less labeling; however, one notion we support is an overall total reduction in PDGFR α expressing cells within WATs. Additional exploration into this hypothesis would be critical for evaluating PDGFR α expression and function in future studies. We also noted, at P10, RFP- cells have about a third of the mRNA of *Pdgfra* than RFP+ cells, indicating not all of the PDGFR α cells underwent DNA recombination under our experimental conditions and labeling efficiency. This low labeling is consistent with a previous study by Jeffery et al, who reported that two different inducible lines of *Pdgfra*^{Cre-ERT2} marked adipose lineage with variable efficiency (Jeffery et al., 2014). In alignment, Rodeheffer and colleagues demonstrated the lack of significant fate mapping of PDGFR α cells to *de novo* adult WAT adipogenesis (Jeffery et al., 2014). Nevertheless, our fate-mapping data using this *Pdgfra*^{Cre-ERT2} transgenic line suggest a previously unanticipated differential labeling and contribution of PDGFR α in WAT development and homeostasis. A likely reason we postulate for the differential contribution of PDGFR α is possibly due to the dynamic expression of PDGFR α between developmental and adult APCs.

A limitation of our studies is that our developmental fate mapping data did not allow us to discriminate whether functionally distinct PDGFR α + cells exist to give rise to white and brown adipocytes, or if there is a common progenitor for all adipocytes in different depots. Recent studies using single-cell RNA-sequencing reveal that distinct subpopulations of APCs in the stromal vascular fraction of WAT are present in both mouse and human adipose tissues (Burl et al., 2018; Gu et al., 2019; Hepler et al., 2018; Merrick et al., 2019; Schwalie et al., 2018; Zhou et al., 2019). It will be of future interest to perform single-cell RNA-sequencing or clonal lineage tracing to examine the heterogeneity PDGFR α + cells and their relationship to other APCs within a single depot.

In summary, our study suggests that PDGFR α signaling plays a key role in adipose tissue development by determining adipose progenitor cell fate and in the regulation of progenitor cell dynamics under HFD challenge. This study expands the current knowledge regarding independent adipose progenitor compartments for WAT formation and maintenance. These data highlight the key roles of the distinct APC and their different regulatory mechanism governing WAT organogenesis and homeostasis. Our results may help to discover the new therapeutic targets for treatment and prevention of both childhood and adult obesity, and the subsequent metabolic dysregulation.

4. Materials and Methods

4.1. Animals

All animals were maintained under the guidelines of the University of Illinois at Chicago (UIC) Animal Care and Use Committee. Mice were housed in a 14:10 light:dark cycle, and experimental diets and water were provided *ad libitum*. AdipoTrak mice are defined as *Pparg*^{TA}; TRE-Cre (JAX Stock: 006234); TRE-*H2B-GFP* as previously reported (Tang et al., 2008). *Rosa26R*^{RFP} (JAX Stock No: 007908), *Pdgfra*^{Cre} (JAX Stock No: 013148), *Pparg*^{fl/fl} (JAX Stock No: 004584), and *Pdgfra*^{fl/fl} (JAX Stock No: 006492) mice were obtained from the Jackson

Laboratory. *Acta2*^{Cre-ERT2} mice were generously provided by Dr. Pierre Chambon. Drs. Sean Morrison and Bill Richardson generously provided the *Pdgfra*^{Cre-ERT2}. Cre recombination was induced by administering one dose of tamoxifen (Cayman, Ann Arbor, MI) dissolved in sunflower oil (Sigma-Aldrich, St. Louis, MO) for one or two consecutive days (50mg/Kg intraperitoneal injection). In these experiments, tamoxifen was given to all animal groups including control mice which carried the floxed alleles but lacked the *Cre* transgene. For Cre induction in cell culture system, we used 2 uM/mL 4-hydroxytamoxifen (4-OH-tamoxifen, Sigma, Sigma-Aldrich, St. Louis, MO). For cold, mice were placed in a 6.5°C cold metabolic chamber for seven days. The mice were fed either normal chow (4% Kcal fat, Harlan-Teklad, Madison, WI) or high-fat diet (HFD; 60% Kcal fat; D12492, Research Diets, New Brunswick, NJ). Rosi intake was estimated to be 15 mg/kg body mass/day.

4.2. Stromal Vascular Fraction Isolation and Cell Culture

Stromal vascular (SV) cells were isolated from subcutaneous WAT, including inguinal and interscapular depots. After 1 hour of slow shaking of the tissue in isolation buffer (100 mM HEPES pH 7.4, 120 mM NaCl, 50 mM KCl, 5mM Glucose, 1 mM CaCl₂, and 1.5% BSA) containing 1 mg/mL Collagenase, Type 1 (Worthington Biochemical Corporation, Lakewood, NJ) at 37 °C, the suspension was centrifuged at 1000 X g for 10 minutes. The floating adipocyte layer and the solution were removed, and the SV pellet was resuspended in DMEM/F12 media (Sigma-Aldrich, St. Louis, MO) supplemented with 10% FBS (Sigma-Aldrich, St. Louis, MO) and 1% Penicillin/Streptomycin (Gibco, Waltham, MA).

The isolated mouse SV cells were cultured in DMEM/F12 media (Sigma-Aldrich, St. Louis, MO) supplemented with 10% FBS (Sigma-Aldrich, St. Louis, MO) and 1% Penicillin/Streptomycin (Gibco, Waltham, MA). White adipogenesis was induced by treating confluent cells with DMEM/F12 containing 10% FBS, 1 µg/mL insulin (Sigma-Aldrich, St. Louis, MO), 1 µM dexamethasone (Cayman, Ann Arbor, MI), and 0.5mM isobutylmethylxanthine

(Sigma-Aldrich, St. Louis, MO) for the first 3 days and with DMEM/F12 containing 10% FBS and 1 µg/mL insulin for another 3 days.

4.3. Flow Cytometry

SV cells were isolated, washed, centrifuged at 1000 X g for 10 minutes, and sorted with a MoFlo Astrios Cell Sorter (Beckman Coulter, Brea, CA) operated by the UIC Flow Cytometry Core. For RFP+ sorting, live SV cells from P10 and P60 tamoxifen-injected *Pdgfra*^{Cre-ERT2}; *Rosa26R*^{RFP} mice were stained with DAPI to exclude dead cells and sorted based on native fluorescence. The SV cells from RFP- mice were used to determine background fluorescence levels. For GFP+ and RFP+ flow analysis, SV cells were isolated from *Pparg*^{ITA}; TRE-H2B-GFP; *Pdgfra*^{Cre-ERT2}; *Rosa26R*^{RFP} double reporter mice (IGW, PGW and BAT were pooled from n=10 for P10 and n=8 for P60 mice). For GFP+ (native fluorescence)/CD31+ flow analysis, SV cells were isolated from P30 Control and AT-PDGFRα-KO mice. SV cells were stained with rat anti-CD31 (CD31;1:200 BD Bioscience: item no: 550274) on ice for 30 min. Cells were then washed twice with the staining buffer and incubated with cy5 donkey anti-rat (1:500, Jackson ImmunoResearch, item no: 711-605-152) secondary antibody for CD31. Cells were incubated for 30 min on ice before flow cytometric analysis. For gating strategies of both GFP sorting and flow analysis, live cells were selected by size on the basis of FSC and SSC. Single cells were then gated on both SSC and FSC Width singlet's. SVF cells isolated from GFP-negative mice, along with primary-minus-one controls, were used as a negative control to determine background fluorescence levels.

4.4. Quantitative Real-time PCR

Total RNA was extracted using TRIzol (Invitrogen, Carlsbad, CA) from either mouse tissues or cells. cDNA was synthesized using High Capacity RNA to cDNA Kit (Life Technologies, Carlsbad, CA), and gene expression was analyzed using Power SYBR Green PCR Master Mix

with ViiA7 Real-time PCR System (Applied Biosystems, Foster City, CA). Quantitative PCR values were normalized to 18s rRNA expression. Primer sequences are provided in **Table S1**.

4.5. Histological Staining

Hematoxylin and eosin (H&E) or trichrome staining was carried out on paraffin sections using the following procedure. Adipose tissues were fixed in 10% formalin overnight, processed in STP120 tissue processing unit (Thermo-Fisher Scientific, Waltham, MA) in a series of ethanol dehydrated steps (50%, 70%, 80%, 95%, 95%, 100%, and 100% at 45 minutes/step) and xylene substitute rinse steps (3 times, 45 minutes/step), and then submerged in paraffin (2 times, 1 hour/step). Processed tissues were embedded in paraffin blocks using a HistoStar™ tissue embedding station (Thermo-Fisher Scientific, Waltham, MA), and the embedded tissues were sectioned with a HM325 microtome (Thermo-Fisher Scientific, Waltham, MA) at 8 to 12 µm thickness. Slides were baked for 1 hour at 55 °C and stained with H&E. For immunohistochemistry (IHC), sections were deparaffinized, boiled in antigen-retrieval solution, treated with UCP1 antibody (1:500, ab23841, Abcam, Cambridge, United Kingdom), and stained with Vectastain ABC KIT (PK-6100, Vector Laboratories, Burlingame, CA) and DAB KIT (SK-4100, Vector Laboratories, Burlingame, CA). RFP (tdTomato) reporter expression in paraffin sections was visualized by immunostaining with a mouse monoclonal antibody against DsRed (Takara, 632392) at 1:500. Adipocytes were identified by immunostaining with anti-Perilipin-1 (Abcam, ab61682) used at 1:1000. To stain lipid, chopped adipose tissues were incubated in LipidTox (Invitrogen, Carlsbad, CA) at 1:200 in PBS for overnight at 4 °C before washing in 1X PBS and mounting for imaging. Whole-mount images were taken on a Leica M205 FA microscope, and immunostaining images were collected on a Leica DMI8 inverted microscope. For quantification of images, two independent observers assessed 3 random fields in 10 random sections from at least 3 mice per cohort.

4.6. Oil Red O Staining

In vitro differentiated cells were fixed in 4% paraformaldehyde for 45 minutes at room temperature. After washing with 1X PBS twice, cells were stained with Oil Red O working solution (0.5% isopropanol, Sigma-Aldrich, St. Louis, MO) at room temperature for 30 minutes. The Oil Red O solution was removed, and cells were washed with 1X PBS before imaging.

4.7. Metabolic Phenotyping Experiments

Temperature was monitored daily using a rectal probe (Physitemp). The probe was lubricated with glycerol and was inserted 1.27 cm (0.5 in), and temperature was measured when stabilized. Body composition was measured using a Bruker minispec 10 whole body composition analyzer (Bruker, Billerica, MA) at UIC Biologic Resources Laboratory. For glucose monitoring, tail blood was drawn in the morning and blood glucose levels were measured with a Contour glucometer (Bayer, Leverkusen, Germany). For glucose tolerance tests, 1.25mg glucose/g body weight of mouse was injected intraperitoneally after a 5-hour fasting, and blood glucose levels were measured at the indicated intervals.

4.8 Metabolic Cage Studies

Control and SMA-PDGFR α -KO mice were housed individually and acclimatized to the metabolic chambers at UIC Biologic Resources Laboratory for 2 days before data collection was initiated. For the subsequent 3 days, food intake, VO₂, VCO₂, and physical activity were monitored over a 12 hour light/dark cycle with food provided ad libitum.

4.9. Quantification and Statistical Analysis

All labeling quantifications were performed in at least 4 animals, with a minimal of 3 distinct sections being imaged and counted per animal. Two-tailed Student's t-test or one-way ANOVA followed by post-hoc comparisons using Bonferroni post-hoc test was conducted. $P < 0.05$ was

considered statistically significant. Data were presented as mean \pm standard error of mean (SEM) and plotted in GraphPad Prism 8.0. All experiments were performed on 2 to 3 independent cohorts with a minimum of 4 mice/group.

ACKNOWLEDGMENTS

We thank Dr. Jonathan M Graff for supporting this work and giving fruitful advice. We thank Dr. Pierre Chambon for the *Acta2*^{Cre-ERT2} mouse strain. We thank Cynthia Rose Adams and Jeanette Purcell for assistance with mouse husbandry, Stefan J. Green and the Research Resources Center for quantitative real-time PCR analysis, Dr. Brian Layden and Metabolic Phenotyping Core for analytical and phenotypical mouse measurements, Balaji Ganesh and Flow Cytometry Core facility for FACS and members of the Jiang laboratory for helpful comments on the manuscript. This work is supported by the National Institute of Diabetes and Digestive and Kidney Disease grant K01 DK111771 and Pilot & Feasibility Diabetes Research & Training Center (DRTC) Award (P30DK020595).

5. References

- Berry, D.C., Jiang, Y., and Graff, J.M. (2016a). Emerging Roles of Adipose Progenitor Cells in Tissue Development, Homeostasis, Expansion and Thermogenesis. *Trends Endocrinol Metab* 27, 574-585.
- Berry, D.C., Jiang, Y., and Graff, J.M. (2016b). Mouse strains to study cold-inducible beige progenitors and beige adipocyte formation and function. *Nat Commun* 7, 10184.
- Berry, D.C., Stenesen, D., Zeve, D., and Graff, J.M. (2013). The developmental origins of adipose tissue. *Development* 140, 3939-3949.
- Berry, R., Jeffery, E., and Rodeheffer, M.S. (2014). Weighing in on adipocyte precursors. *Cell Metab* 19, 8-20.
- Berry, R., and Rodeheffer, M.S. (2013). Characterization of the adipocyte cellular lineage in vivo. *Nat Cell Biol* 15, 302-308.
- Burl, R.B., Ramseyer, V.D., Rondini, E.A., Pique-Regi, R., Lee, Y.H., and Granneman, J.G. (2018). Deconstructing Adipogenesis Induced by beta3-Adrenergic Receptor Activation with Single-Cell Expression Profiling. *Cell Metab* 28, 300-309 e304.
- Cattaneo, P., Mukherjee, D., Spinozzi, S., Zhang, L., Larcher, V., Stallcup, W.B., Kataoka, H., Chen, J., Dimmeler, S., Evans, S.M., et al. (2020). Parallel Lineage-Tracing Studies Establish Fibroblasts as the Prevailing In Vivo Adipocyte Progenitor. *Cell Rep* 30, 571-582 e572.
- Cawthorn, W.P., Scheller, E.L., and MacDougald, O.A. (2012). Adipose tissue stem cells meet preadipocyte commitment: going back to the future. *J Lipid Res* 53, 227-246.
- Crossno, J.T., Jr., Majka, S.M., Grazia, T., Gill, R.G., and Klemm, D.J. (2006). Rosiglitazone promotes development of a novel adipocyte population from bone marrow-derived circulating progenitor cells. *J Clin Invest* 116, 3220-3228.
- Ding, G., Tanaka, Y., Hayashi, M., Nishikawa, S., and Kataoka, H. (2013). PDGF receptor alpha+ mesoderm contributes to endothelial and hematopoietic cells in mice. *Dev Dyn* 242, 254-268.
- Farmer, S.R. (2006). Transcriptional control of adipocyte formation. *Cell Metab* 4, 263-273.
- Gao, Z., Daquinag, A.C., Su, F., Snyder, B., and Kolonin, M.G. (2018). PDGFRalpha/PDGFRbeta signaling balance modulates progenitor cell differentiation into white and beige adipocytes. *Development* 145.
- Ginsberg-Fellner, F. (1981). Growth of adipose tissue in infants, children and adolescents: variations in growth disorders. *Int J Obes* 5, 605-611.
- Gu, W., Nowak, W.N., Xie, Y., Le Bras, A., Hu, Y., Deng, J., Issa Bhaloo, S., Lu, Y., Yuan, H., Fidanis, E., et al. (2019). Single-Cell RNA-Sequencing and Metabolomics Analyses Reveal the Contribution of Perivascular Adipose Tissue Stem Cells to Vascular Remodeling. *Arterioscler Thromb Vasc Biol* 39, 2049-2066.

638 Gupta, R.K., Mepani, R.J., Kleiner, S., Lo, J.C., Khandekar, M.J., Cohen, P., Frontini, A.,
639 Bhowmick, D.C., Ye, L., Cinti, S., et al. (2012). Zfp423 expression identifies committed
640 preadipocytes and localizes to adipose endothelial and perivascular cells. *Cell Metab* 15, 230-
641 239.

642 Hajer, G.R., van Haeften, T.W., and Visseren, F.L. (2008). Adipose tissue dysfunction in
643 obesity, diabetes, and vascular diseases. *Eur Heart J* 29, 2959-2971.

644 Hepler, C., Shan, B., Zhang, Q., Henry, G.H., Shao, M., Vishvanath, L., Ghaben, A.L., Mobley,
645 A.B., Strand, D., Hon, G.C., et al. (2018). Identification of functionally distinct fibro-inflammatory
646 and adipogenic stromal subpopulations in visceral adipose tissue of adult mice. *Elife* 7.

647 Hepler, C., Vishvanath, L., and Gupta, R.K. (2017). Sorting out adipocyte precursors and their
648 role in physiology and disease. *Genes Dev* 31, 127-140.

649 Hirsch, J., and Batchelor, B. (1976). Adipose tissue cellularity in human obesity. *Clin Endocrinol*
650 *Metab* 5, 299-311.

651 Hirsch, J., and Knittle, J.L. (1970). Cellularity of obese and nonobese human adipose tissue.
652 *Fed Proc* 29, 1516-1521.

653 Iwayama, T., Steele, C., Yao, L., Dozmorov, M.G., Karamichos, D., Wren, J.D., and Olson, L.E.
654 (2015). PDGFRalpha signaling drives adipose tissue fibrosis by targeting progenitor cell
655 plasticity. *Genes Dev* 29, 1106-1119.

656 Jeffery, E., Berry, R., Church, C.D., Yu, S., Shook, B.A., Horsley, V., Rosen, E.D., and
657 Rodeheffer, M.S. (2014). Characterization of Cre recombinase models for the study of adipose
658 tissue. *Adipocyte* 3, 206-211.

659 Jeffery, E., Church, C.D., Holtrup, B., Colman, L., and Rodeheffer, M.S. (2015). Rapid depot-
660 specific activation of adipocyte precursor cells at the onset of obesity. *Nat Cell Biol* 17, 376-385.

661 Jiang, Y., Berry, D.C., and Graff, J. (2017a). Distinct cellular and molecular mechanisms for
662 beta3 adrenergic receptor induced beige adipocyte formation. *Elife* 6.

663 Jiang, Y., Berry, D.C., Jo, A., Tang, W., Arpke, R.W., Kyba, M., and Graff, J.M. (2017b). A
664 PPARgamma transcriptional cascade directs adipose progenitor cell-niche interaction and niche
665 expansion. *Nat Commun* 8, 15926.

666 Jiang, Y., Berry, D.C., Tang, W., and Graff, J.M. (2014). Independent stem cell lineages
667 regulate adipose organogenesis and adipose homeostasis. *Cell Rep* 9, 1007-1022.

668 Jiang, Y., Jo, A.Y., and Graff, J.M. (2012a). SnapShot: adipocyte life cycle. *Cell* 150, 234-234
669 e232.

670 Jiang, Y., Jo, A.Y., and Graff, J.M. (2012b). SnapShot: adipocyte life cycle. *Cell* 150, 234-
671 234.e232.

672 Jo, J., Gavrilova, O., Pack, S., Jou, W., Mullen, S., Sumner, A.E., Cushman, S.W., and Periwai,
673 V. (2009). Hypertrophy and/or Hyperplasia: Dynamics of Adipose Tissue Growth. *PLoS Comput*
674 *Biol* 5, e1000324.

675 Joe, A.W., Yi, L., Natarajan, A., Le Grand, F., So, L., Wang, J., Rudnicki, M.A., and Rossi, F.M.
676 (2010). Muscle injury activates resident fibro/adipogenic progenitors that facilitate myogenesis.
677 *Nat Cell Biol* 12, 153-163.

678 Kershaw, E.E., and Flier, J.S. (2004). Adipose tissue as an endocrine organ. *J Clin Endocrinol*
679 *Metab* 89, 2548-2556.

680 Knittle, J.L., Timmers, K., Ginsberg-Fellner, F., Brown, R.E., and Katz, D.P. (1979). The growth
681 of adipose tissue in children and adolescents. Cross-sectional and longitudinal studies of
682 adipose cell number and size. *J Clin Invest* 63, 239-246.

683 Lee, K.Y., Luong, Q., Sharma, R., Dreyfuss, J.M., Ussar, S., and Kahn, C.R. (2019).
684 Developmental and functional heterogeneity of white adipocytes within a single fat depot. *EMBO*
685 *J* 38.

686 Lee, M.J., Wu, Y., and Fried, S.K. (2013a). Adipose tissue heterogeneity: implication of depot
687 differences in adipose tissue for obesity complications. *Mol Aspects Med* 34, 1-11.

688 Lee, Y.-H., Petkova, A.P., Mottillo, E.P., and Granneman, J.G. (2012a). In vivo identification of
689 bipotential adipocyte progenitors recruited by β 3-adrenoceptor activation and high-fat feeding.
690 *Cell metabolism* 15, 480-491.

691 Lee, Y.H., Petkova, A.P., and Granneman, J.G. (2013b). Identification of an adipogenic niche
692 for adipose tissue remodeling and restoration. *Cell Metab* 18, 355-367.

693 Lee, Y.H., Petkova, A.P., Mottillo, E.P., and Granneman, J.G. (2012b). In vivo identification of
694 bipotential adipocyte progenitors recruited by beta3-adrenoceptor activation and high-fat
695 feeding. *Cell Metab* 15, 480-491.

696 Lehrke, M., and Lazar, M.A. (2005). The many faces of PPARgamma. *Cell* 123, 993-999.

697 Marcelin, G., Ferreira, A., Liu, Y., Atlan, M., Aron-Wisnewsky, J., Pelloux, V., Botbol, Y.,
698 Ambrosini, M., Fradet, M., Rouault, C., et al. (2017). A PDGFRalpha-Mediated Switch toward
699 CD9(high) Adipocyte Progenitors Controls Obesity-Induced Adipose Tissue Fibrosis. *Cell Metab*
700 25, 673-685.

701 Merrick, D., Sakers, A., Irgebay, Z., Okada, C., Calvert, C., Morley, M.P., Percec, I., and Seale,
702 P. (2019). Identification of a mesenchymal progenitor cell hierarchy in adipose tissue. *Science*
703 364.

704 Rigamonti, A., Brennand, K., Lau, F., and Cowan, C.A. (2011). Rapid cellular turnover in
705 adipose tissue. *PLoS One* 6, e17637.

706 Rivera-Gonzalez, G.C., Shook, B.A., Andrae, J., Holtrup, B., Bollag, K., Betsholtz, C.,
707 Rodeheffer, M.S., and Horsley, V. (2016). Skin Adipocyte Stem Cell Self-Renewal Is Regulated
708 by a PDGFA/AKT-Signaling Axis. *Cell Stem Cell* 19, 738-751.

709 Rivers, L.E., Young, K.M., Rizzi, M., Jamen, F., Psachoulia, K., Wade, A., Kessar, N., and
710 Richardson, W.D. (2008). PDGFRA/NG2 glia generate myelinating oligodendrocytes and
711 piriform projection neurons in adult mice. *Nat Neurosci* 11, 1392-1401.

712 Rosen, E.D., and Spiegelman, B.M. (2006). Adipocytes as regulators of energy balance and
713 glucose homeostasis. *Nature* **444**, 847-853.

714 Rosen, E.D., and Spiegelman, B.M. (2014). What we talk about when we talk about fat. *Cell*
715 **156**, 20-44.

716 Sanchez-Gurmaches, J., and Guertin, D.A. (2014). Adipocytes arise from multiple lineages that
717 are heterogeneously and dynamically distributed. *Nat Commun* **5**, 4099.

718 Sanchez-Gurmaches, J., Hsiao, W.Y., and Guertin, D.A. (2015). Highly selective in vivo labeling
719 of subcutaneous white adipocyte precursors with Prx1-Cre. *Stem Cell Reports* **4**, 541-550.

720 Schwalie, P.C., Dong, H., Zachara, M., Russeil, J., Alpern, D., Akchiche, N., Caprara, C., Sun,
721 W., Schlaudraff, K.U., Soldati, G., et al. (2018). A stromal cell population that inhibits
722 adipogenesis in mammalian fat depots. *Nature* **559**, 103-108.

723 Sebo, Z.L., Jeffery, E., Holtrup, B., and Rodeheffer, M.S. (2018). A mesodermal fate map for
724 adipose tissue. *Development* **145**.

725 Sebo, Z.L., and Rodeheffer, M.S. (2019). Assembling the adipose organ: adipocyte lineage
726 segregation and adipogenesis in vivo. *Development* **146**.

727 Shao, M., Hepler, C., Vishvanath, L., MacPherson, K.A., Busbuso, N.C., and Gupta, R.K.
728 (2017). Fetal development of subcutaneous white adipose tissue is dependent on Zfp423. *Mol*
729 *Metab* **6**, 111-124.

730 Smorlesi, A., Frontini, A., Giordano, A., and Cinti, S. (2012). The adipose organ: white-brown
731 adipocyte plasticity and metabolic inflammation. *Obes Rev* **13 Suppl 2**, 83-96.

732 Spalding, K.L., Arner, E., Westermarck, P.O., Bernard, S., Buchholz, B.A., Bergmann, O.,
733 Blomqvist, L., Hoffstedt, J., Naslund, E., Britton, T., et al. (2008). Dynamics of fat cell turnover in
734 humans. *Nature* **453**, 783-787.

735 Spiegelman, B.M., and Flier, J.S. (2001). Obesity and the regulation of energy balance. *Cell*
736 **104**, 531-543.

737 Sun, C., Berry, W.L., and Olson, L.E. (2017). PDGFRalpha controls the balance of stromal and
738 adipogenic cells during adipose tissue organogenesis. *Development* **144**, 83-94.

739 Tang, W., Zeve, D., Seo, J., Jo, A.Y., and Graff, J.M. (2011). Thiazolidinediones regulate
740 adipose lineage dynamics. *Cell Metab* **14**, 116-122.

741 Tang, W., Zeve, D., Suh, J.M., Bosnakovski, D., Kyba, M., Hammer, R.E., Tallquist, M.D., and
742 Graff, J.M. (2008). White fat progenitor cells reside in the adipose vasculature. *Science* **322**,
743 583-586.

744 Tran, K.V., Gealekman, O., Frontini, A., Zingaretti, M.C., Morroni, M., Giordano, A., Smorlesi,
745 A., Perugini, J., De Matteis, R., Sbarbati, A., et al. (2012). The vascular endothelium of the
746 adipose tissue gives rise to both white and brown fat cells. *Cell Metab* **15**, 222-229.

747 Trayhurn, P., and Beattie, J.H. (2001). Physiological role of adipose tissue: white adipose tissue
748 as an endocrine and secretory organ. *Proc Nutr Soc* 60, 329-339.

749 Vishvanath, L., MacPherson, K.A., Hepler, C., Wang, Q.A., Shao, M., Spurgin, S.B., Wang,
750 M.Y., Kusminski, C.M., Morley, T.S., and Gupta, R.K. (2015). Pdgfrbeta Mural Preadipocytes
751 Contribute to Adipocyte Hyperplasia Induced by High-Fat-Diet Feeding and Prolonged Cold
752 Exposure in Adult Mice. *Cell Metab*.

753 Vishvanath, L., MacPherson, K.A., Hepler, C., Wang, Q.A., Shao, M., Spurgin, S.B., Wang,
754 M.Y., Kusminski, C.M., Morley, T.S., and Gupta, R.K. (2016). Pdgfrbeta(+) Mural Preadipocytes
755 Contribute to Adipocyte Hyperplasia Induced by High-Fat-Diet Feeding and Prolonged Cold
756 Exposure in Adult Mice. *Cell Metab* 23, 350-359.

757 Wang, Q.A., Tao, C., Gupta, R.K., and Scherer, P.E. (2013). Tracking adipogenesis during
758 white adipose tissue development, expansion and regeneration. *Nat Med* 19, 1338-1344.

759 Wang, Q.A., Tao, C., Jiang, L., Shao, M., Ye, R., Zhu, Y., Gordillo, R., Ali, A., Lian, Y., Holland,
760 W.L., et al. (2015). Distinct regulatory mechanisms governing embryonic versus adult adipocyte
761 maturation. *Nat Cell Biol* 17, 1099-1111.

762 Ye, R., Wang, Q.A., Tao, C., Vishvanath, L., Shao, M., McDonald, J.G., Gupta, R.K., and
763 Scherer, P.E. (2015). Impact of tamoxifen on adipocyte lineage tracing: Inducer of adipogenesis
764 and prolonged nuclear translocation of Cre recombinase. *Mol Metab* 4, 771-778.

765 Zhou, W., Lin, J., Zhao, K., Jin, K., He, Q., Hu, Y., Feng, G., Cai, Y., Xia, C., Liu, H., et al.
766 (2019). Single-Cell Profiles and Clinically Useful Properties of Human Mesenchymal Stem Cells
767 of Adipose and Bone Marrow Origin. *Am J Sports Med* 47, 1722-1733.

768

769

Figure Legends:

Figure 1. Developmental, but not adult, adipocytes derive from a PDGFR α + cell source.

(A-B) *Pdgfra*^{Cre-ERT2}; *Rosa26R*^{RFP} (PDGFR α -RFP) mice were administered tamoxifen (TM) (A) at post-natal day (P) 10 and fed chow or HFD until P60 or (B) at P60 and fed chow or HFD until P120. IGW, PGW and BATs were examined for direct RFP fluorescence either at (A) P60 or (B) P120 (chase). White arrowheads indicate the epididymis labeling. Scale = 100 μ m.
(C-D) RFP staining of IGW, PGW and BATs from above P10-P60 and P60-P120 mice using immunohistochemistry (IHC). Scale = 200 μ m.

Figure 2. Developmental, but not adult, PDGFR α + cells are adipogenic.

(A-B) *Pdgfra*^{Cre-ERT2}; *Rosa26R*^{RFP} (PDGFR α -RFP) male mice were administered TM at P10 (A) or P60 (B). Stromal vascular fraction of cells (SVF) were isolated from IGW of the mice after 3 days and cultured. The numbers indicate the percentage of the RFP+ labeled adipocytes. Scale = 100 μ m.
(C) TM-induced PDGFR α -RFP male mice either at P10 or P60 were fed chow or HFD until P120. SVF were isolated from IGW of the mice at P120, cultured, and examined for direct RFP fluorescence. Scale = 100 μ m.
(D) RT-PCR analysis of adipogenic markers from cells described in C. *P<0.05 P10 RFP- compared to P10 RFP+ cells.
(E) Gene expression levels of P10 and P60 RFP+ cells in SVF isolated from pooled IGW (n=10). *P<0.05 P60 RFP+ compared to P10 RFP+ cells. Data are expressed as mean \pm SEM.
(F) *Pparg*^{fl/fl}-H2BGFP; PDGFR α -RFP male mice were administered TM at P10 or P60. SVF were isolated from pooled IGW, PGW and BAT (n=8) after 3 days and sorted using RFP signal. GFP+RFP+ cells were quantified.

Figure 3. Developmental PDGFR α + cells contribute to postnatal but not adult WAT development.

(A) *Pdgfra*^{Cre-ERT2}; *Rosa26R*^{RFP} (PDGFR α -RFP) mice were administered TM (A) at post-natal day (P) 10 and fed chow or HFD until P120. IGW, PGW and BATs were examined for direct RFP fluorescence and RFP IHC staining. Scale = 100 μ m and 200 μ m.
(B) Two- and six-month old PDGFR α -RFP mice were analyzed. IGWs were examined for direct RFP fluorescence and stained with LipidTox (blue). The quantifications for numbers of RFP+ adipocytes were calculated. Scale = 100 μ m.
(C) Two- and six-month old control and *Pdgfra*^{Cre}; *Pparg*^{fl/fl} (PDGFR α -PPAR γ -KO) mice were analyzed. IGWs were examined using hematoxylin and eosin (H&E) staining. Scale = 100 μ m.

Figure 4. Deleting *Pdgfra* in adult SMA+ APCs is dispensable for adult white adipogenesis.

(A-B) *Acta2*^{Cre-ERT2}; *Pdgfra*^{fl/fl} male control and mutant (SMA-PDGFR α -KO) mice were administered TM at P60 and analyzed at P90.
(C) Body weight of control and SMA-PDGFR α -KO mice at P90. Data are expressed as mean \pm SEM.
(D) Adipose tissue weights. Data are expressed as mean \pm SEM.
(E) Blood glucose level during glucose tolerance test. Data are expressed as mean \pm SEM.
(F) Hematoxylin and eosin (H&E) staining of IGW, PGW and BAT. Scale = 100 μ m.
(G) IGW and PGW were analyzed for direct RFP fluorescence and stained with LipidTox. Scale = 200 μ m.

(H) Oil red o staining of SVF adipogenesis from IGW of control and SMA-PDGFR α -KO male mice at P90.

Figure 5. Deleting *Pdgfra* in adult SMA+ APCs is dispensable for cold-induced beige adipogenesis.

(A) Three-month-old *Acta2*^{Cre-ERT2}; *Pdgfra*^{f/f} male control and SMA-PDGFR α -KO mice were administered TM. After 14 days of TM washout, the mice were cold-exposed for 7 days.
(B) Rectal temperature after cold exposure. Data are expressed as mean \pm SEM.
(C) Body weight after cold exposure. Data are expressed as mean \pm SEM.
(D) Blood glucose after cold exposure. Data are expressed as mean \pm SEM.
(E) Adipose tissue weight. Data are expressed as mean \pm SEM.
(F) Hematoxylin and eosin (H&E) staining of IGW and PGW. Scale = 100 μ m.
(G) UCP1 staining of IGW and PGW using immunohistochemistry (IHC). Scale = 100 μ m.

Figure 6. PDGFR α in developmental APCs is essential for adipose tissue development.

(A) Two-month-old *Pparg*^{tTA}; TRE-Cre; TRE-H2B-GFP; *Pdgfra*^{f/f} male control and AT-PDGFR α -KO mice were analyzed.
(B) Body weight. Data are expressed as mean \pm SEM.
(C) IGW and PGW tissue.
(D) Adipose tissue weight. *P<0.05 AT-PDGFR α compared to AT-Con mice. Data are expressed as mean \pm SEM.
(E) Other tissue weight. Data are expressed as mean \pm SEM.
(F) Blood glucose level during glucose tolerance test. *P<0.05 AT-PDGFR α -KO compared to control mice. Data are expressed as mean \pm SEM.
(G) Hematoxylin and eosin (H&E) staining of IGW. Scale = 100 μ m.
(H) Oil Red O staining of SVF isolated from IGW of control and AT-PDGFR α -KO mice.

Figure 7. PDGFR α regulates adipose tissue development through lineage control.

(A) Two-month-old *Pparg*^{tTA}; TRE-Cre; TRE-H2B-GFP; *Pdgfra*^{f/f} male control and AT-PDGFR α -KO mice were analyzed. Trichrome staining of IGW. Scale = 200 μ m
(B) Direct GFP fluorescence of IGW. Scale = 100 μ m.
(C) Flow cytometry profiles of SVF isolated from IGW.
(D) Quantification of GFP+ adipose progenitor cell number. Data are expressed as mean \pm SEM.
(E) Adipogenic marker gene expression levels in GFP+ cells of SVF isolated from IGW. Data are expressed as mean \pm SEM.
(F) Fibrotic marker gene expression levels in GFP+ cells of SVF isolated from IGW. Data are expressed as mean \pm SEM. *P<0.05 AT-PDGFR α -KO compared to control mice in D-F.
(G) Working model for PDGFR α in developmental and adult progenitors. Developmental progenitors are marked by PDGFR α + and adipogenesis is dependent on PDGFR α . In the absence of PDGFR α , developmental progenitors switch the lineage to fibrotic. Adult progenitors for WAT homeostasis are not marked by PDGFR α + and adipogenesis during WAT homeostasis is largely PDGFR α independent.

Figure Supplement Legends:

Figure 1_Figure supplement 1. *Pdgfra*-dependent RFP expression at pulse, P60-P180, and P60-P120 TZD pulse-chase.

(A-B) *Pdgfra*^{Cre-ERT2}; *Rosa26R*^{RFP} (PDGFR α -RFP) mice were administered TM (A) at post-natal day (P) 10 or (B) at P60. IGW, PGW and BATs were examined for direct RFP fluorescence and RFP IHC staining after 3 days (pulse). Scale = 200 μ m.

(C) PDGFR α -RFP mice were administered TM at P60 and fed chow or HFD until P180. IGW, PGW and BATs were examined for direct RFP fluorescence and RFP IHC staining at P180 (chase). Scale = 100 μ m and 200 μ m.

(D) Quantification of RFP+ adipocytes observed in randomly chosen 10X magnification fields from IGW, PGW and BAT sections.

(E) Confocal immunofluorescence image of a representative IGW section from animals treated with TZD.

Sections were stained with anti-RFP (red) and anti-Perilipin(green) antibodies and counterstained with DAPI (blue; nuclei). Scale = 200 μ m .

Figure 2_Figure supplement 1. Developmental, but not adult, PDGFR α + cells overlap with PPAR γ + cells.

(A) Schematic of *Pparg*^{tTA}-*H2BGFP*; PDGFR α -RFP male mice breeding. Mice were administered TM at P10 or P60. SVF were isolated after 3 days. GFP+RFP+ cells were quantified in IGW, PGW and BAT.

(B) The flow analysis of P10 labeled PDGFR α -RFP cells overlapping with *Pparg*^{tTA} labeled GFP+ cells. The numbers indicate the percentage of total SVF in IGW, PGW and BAT (pooled SVF from n=10 mice).

(C) The flow analysis of P60 labeled PDGFR α -RFP cells overlapping with *Pparg*^{tTA} labeled GFP+ cells. The numbers indicate the percentage of total SVF in IGW, PGW and BAT (pooled SVF from n=8 mice)

Figure 3_Figure supplement 1. P10 PDGFR α + cells contribute to postnatal but not adult WAT development.

(A) *Pdgfra*^{Cre-ERT2}; *Rosa26R*^{RFP} (PDGFR α -RFP) mice were administered TM (A) at post-natal day (P) 10 and fed chow or HFD until P120. IGW, PGW and BATs were examined for direct RFP fluorescence. Scale = 100 μ m.

(B) Quantification of RFP+ adipocytes observed in randomly chosen 10X magnification fields from IGW, PGW and BAT sections.

(C) Oil red o staining and gene expression analysis of SVF adipogenesis from IGW of *Pdgfra*^{Cre-ERT2}; *Pparg*^{fl/fl} male mice at P60, either veh or 4-OH-tamoxifen (4-OH-TM) treated. *P<0.05 TM compared to Veh cells. Data are expressed as mean \pm SEM.

Figure 4_Figure supplement 1. SMA-PDGFR α -KO mice do not display abnormal energy expenditure.

(A) Body fat mass of *Acta2*^{Cre-ERT2}; *Pdgfra*^{fl/fl} male control and SMA-PDGFR α -KO mice at P90. Data are expressed as mean \pm SEM.

(B) Food intake of control and SMA-PDGFR α -KO mice. Data are expressed as mean \pm SEM.

(C) RT-PCR analysis of *Pdgfra* level in BAT of control and SMA-PDGFR α -KO mice. *P<0.05 SMA-PDGFR α -KO mice compared to control mice. Data are expressed as mean \pm SEM.

(D) Energy expenditure of control and SMA-PDGFR α -KO mice. Data are expressed as mean \pm SEM.

(E) Oxygen consumption of control and SMA-PDGFR α -KO mice. Data are expressed as mean \pm SEM.

(F) Carbon dioxide production of control and SMA-PDGFR α -KO mice. Data are expressed as mean \pm SEM.

(G) Respiratory exchange ratio of control and SMA-PDGFR α -KO mice. Data are expressed as mean \pm SEM.

Figure 5_Figure supplement 1. Deleting *Pdgfra* in adult SMA+ APCs is dispensable for cold-induced beige adipogenesis.

(A) Three-month-old *Acta2*^{Cre-ERT2}; *Pdgfra*^{f/f} male control and SMA-PDGFR α -KO mice were administered TM. After 14 days of TM washout, the mice were cold-exposed for 7 days. H&E staining of BAT. Scale = 100 μ m.

(B) Thermogenic gene expression levels in control and SMA-PDGFR α -KO IGW. Data are expressed as mean \pm SEM.

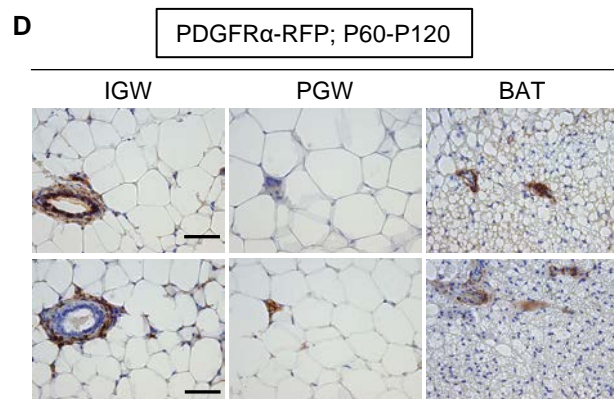
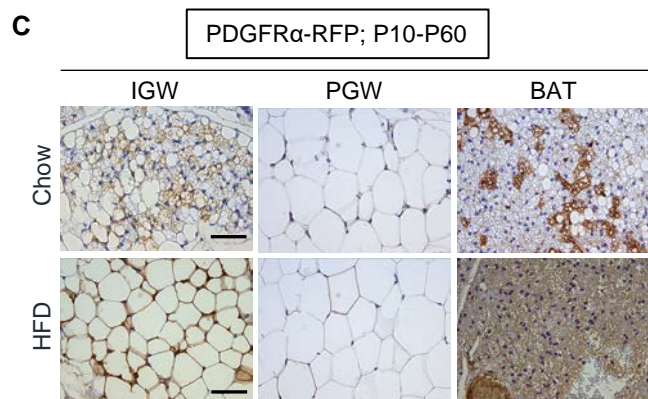
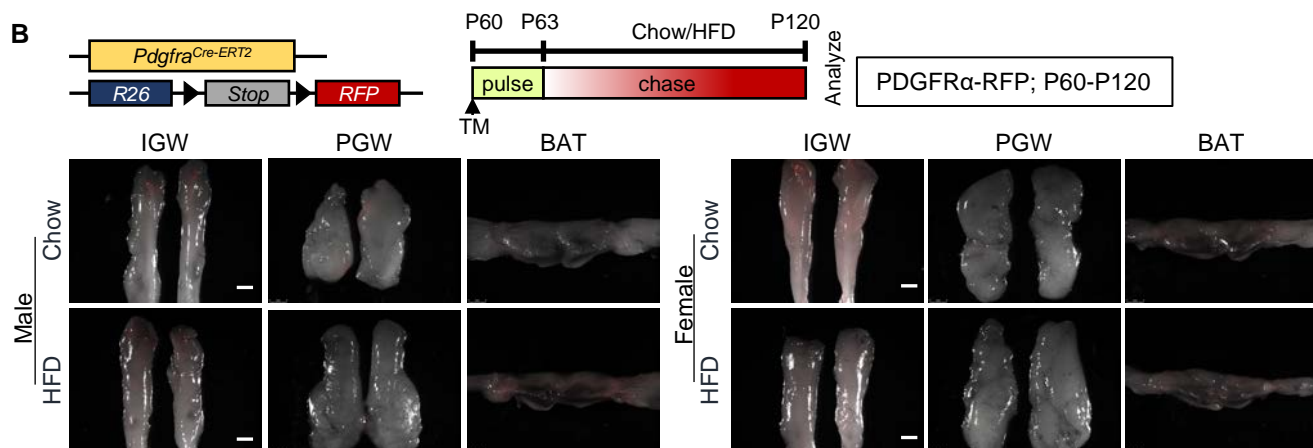
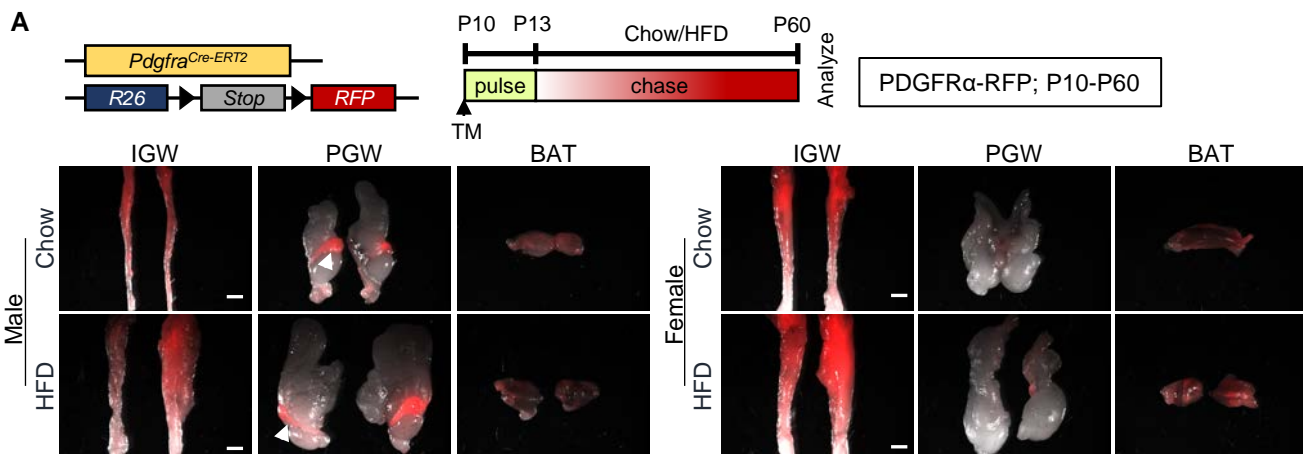
Figure 6_Figure supplement 1. PDGFR α in developmental APCs is essential for adipose tissue development.

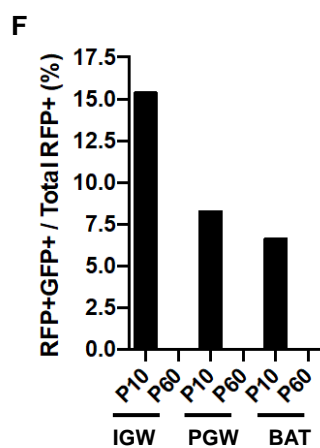
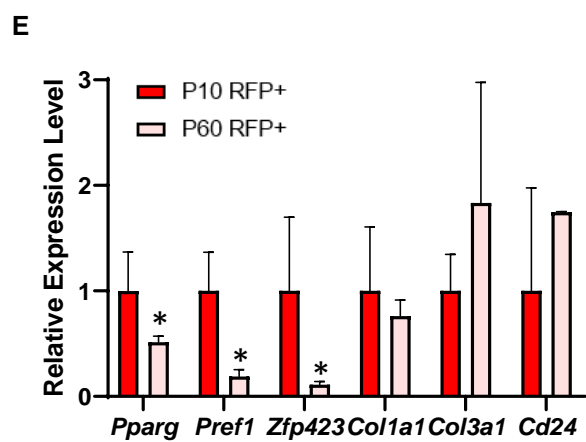
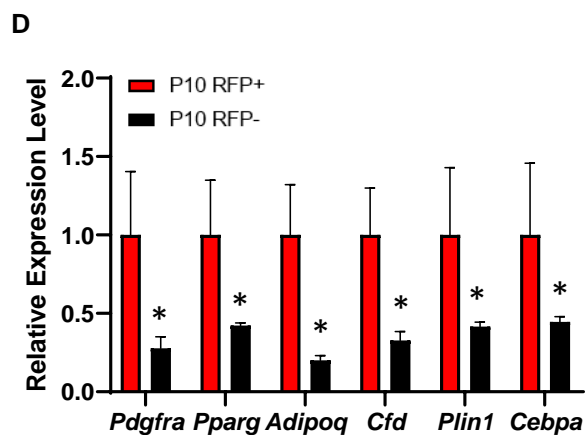
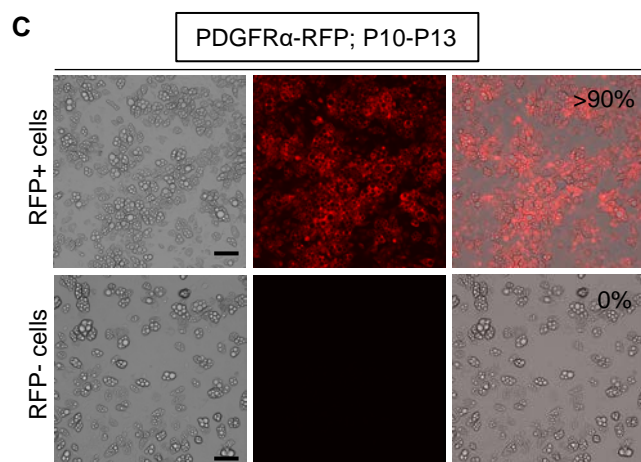
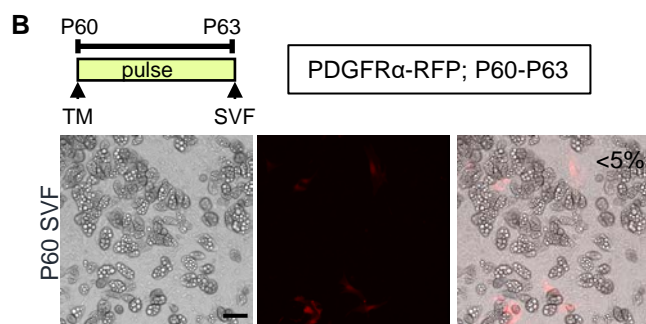
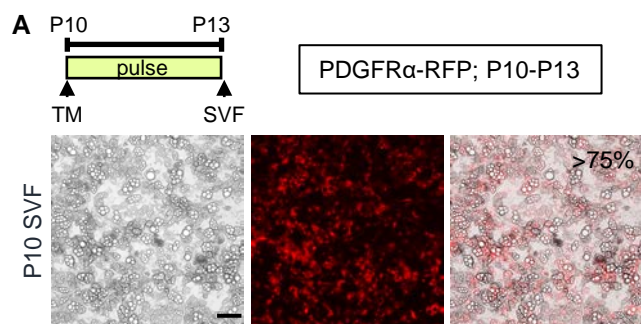
(A) IGW tissues of two-month-old *Pparg*^{tTA}; TRE-Cre; TRE-*H2B-GFP*; *Pdgfra*^{f/f} male control and AT-PDGFR α -KO mice.

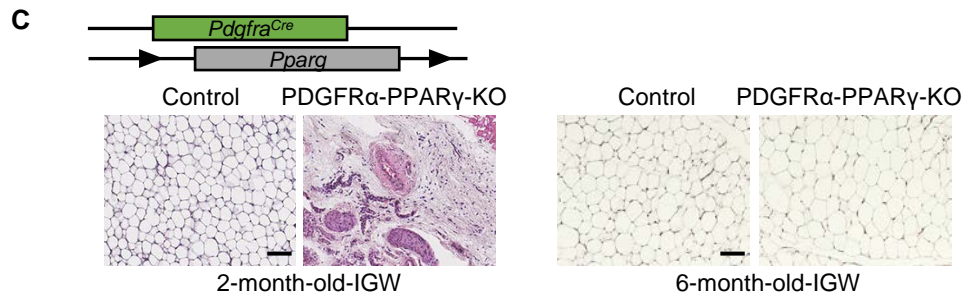
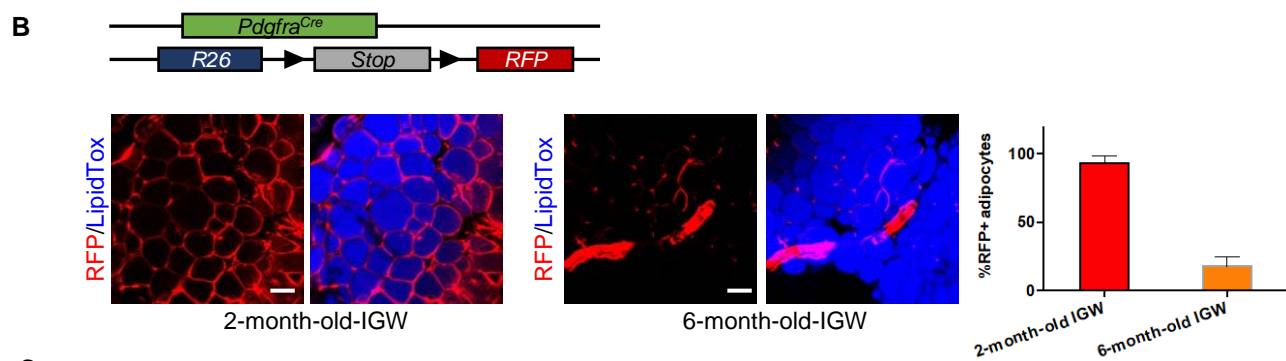
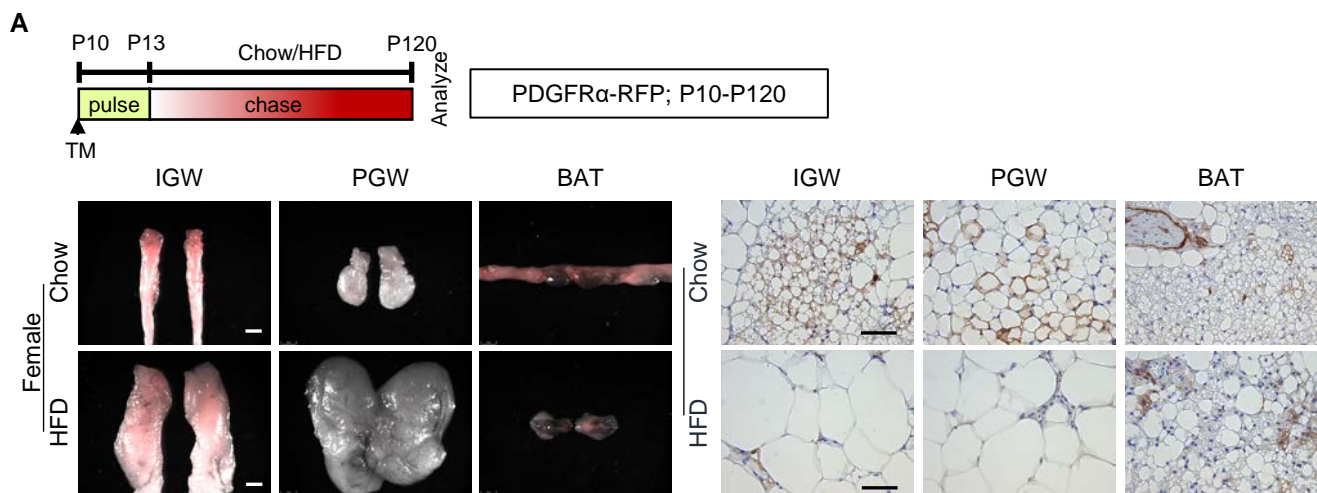
(B) Hematoxylin and eosin (H&E) staining of ISCW and liver of control and AT-PDGFR α -KO mice. Scale = 100 μ m.

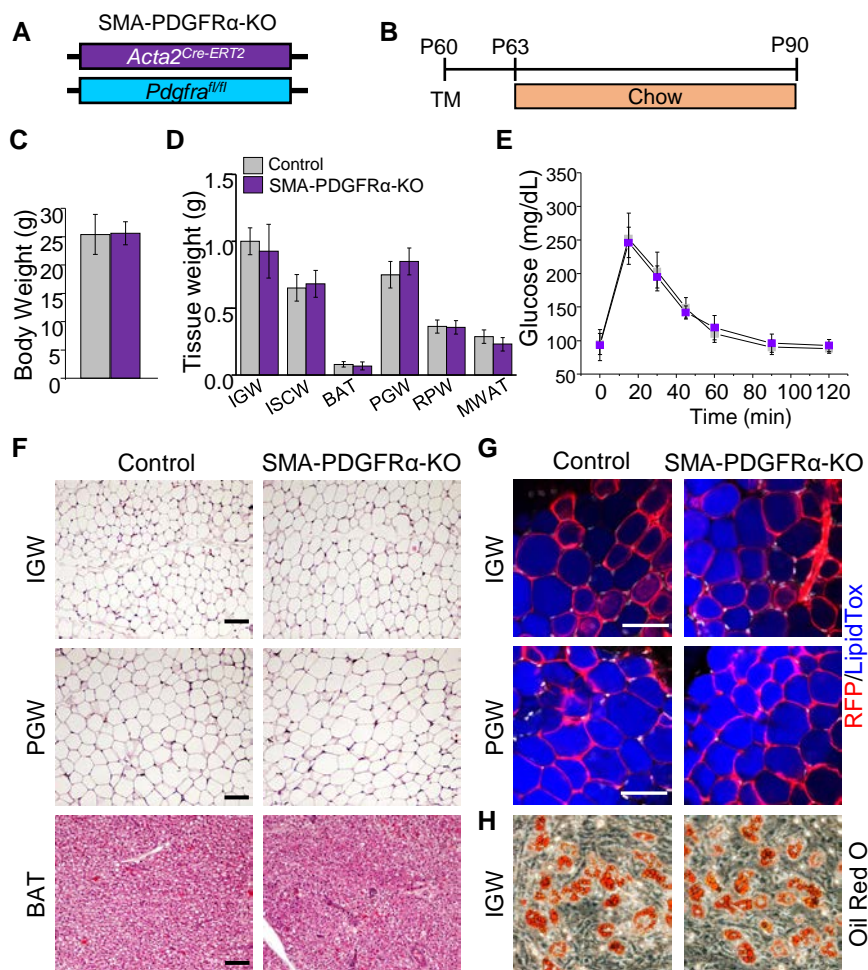
Figure 7_Figure supplement 1. *Pdgfra* deletion in developmental APCs.

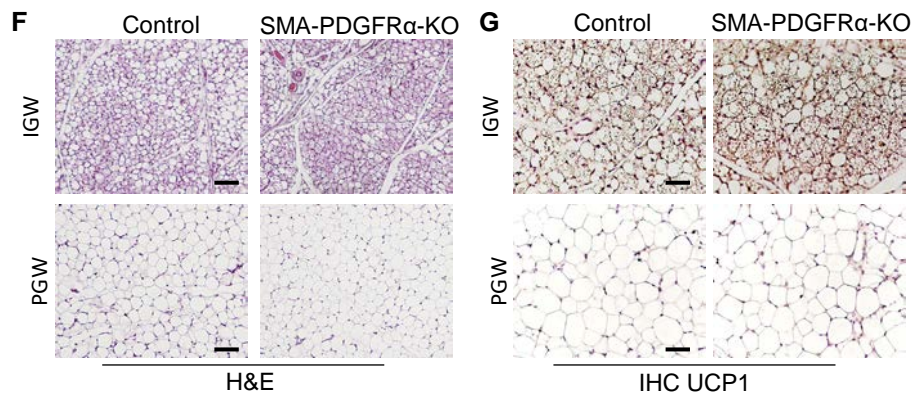
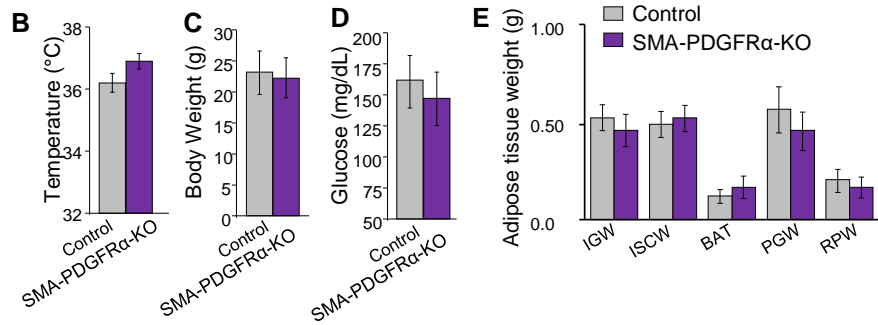
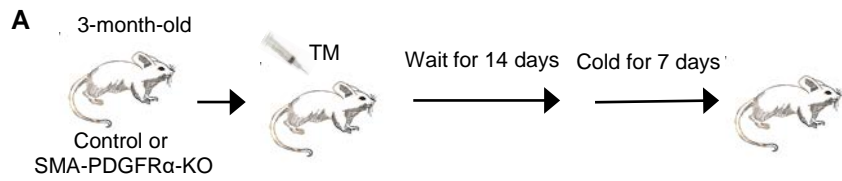
(A) IGW tissues of P60 *Pparg*^{tTA}; TRE-Cre; TRE-*H2B-GFP*; *Pdgfra*^{f/f} male control and AT-PDGFR α -KO mice. White arrowheads indicate the GFP+ progenitors align on the vasculature.

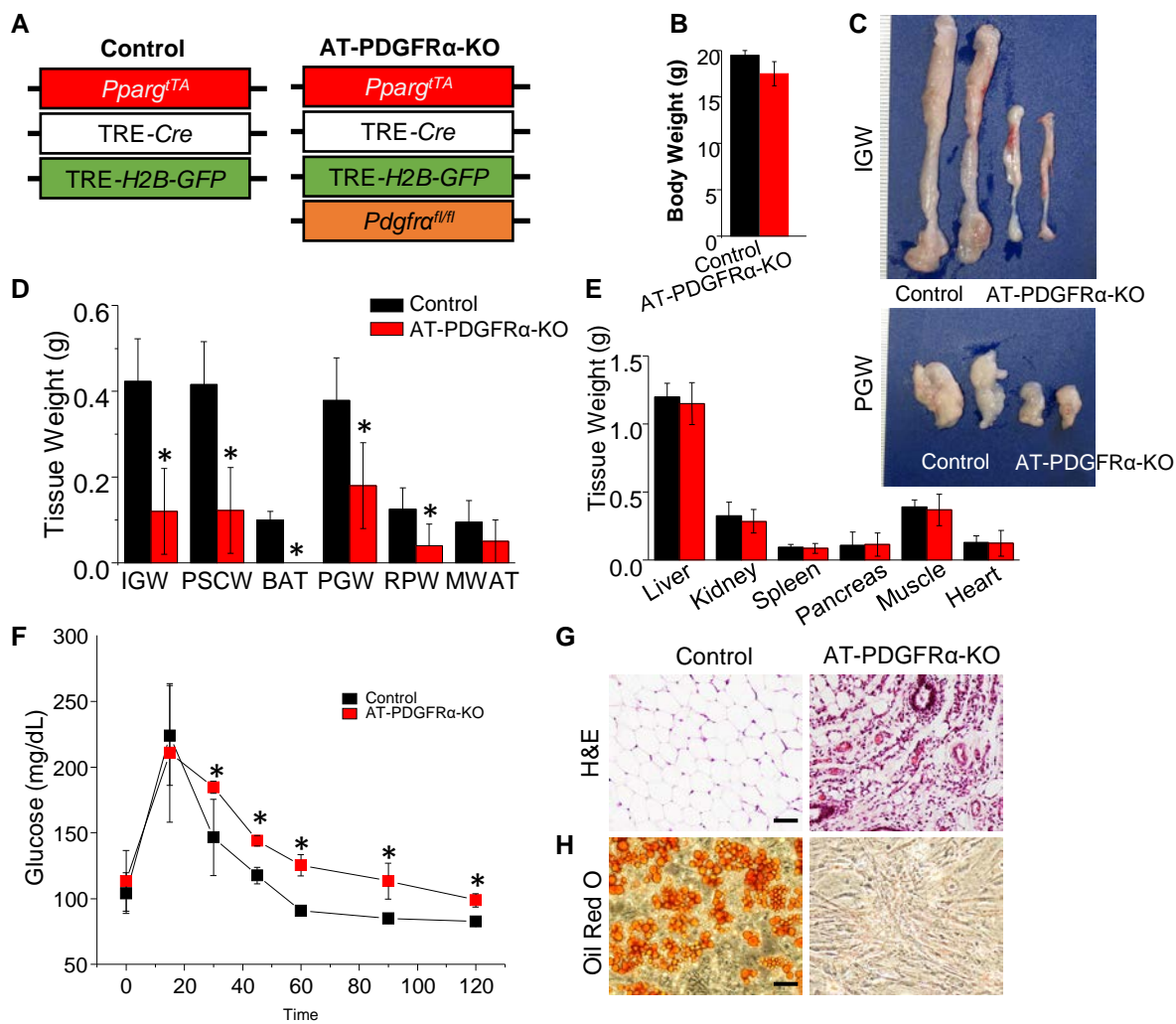


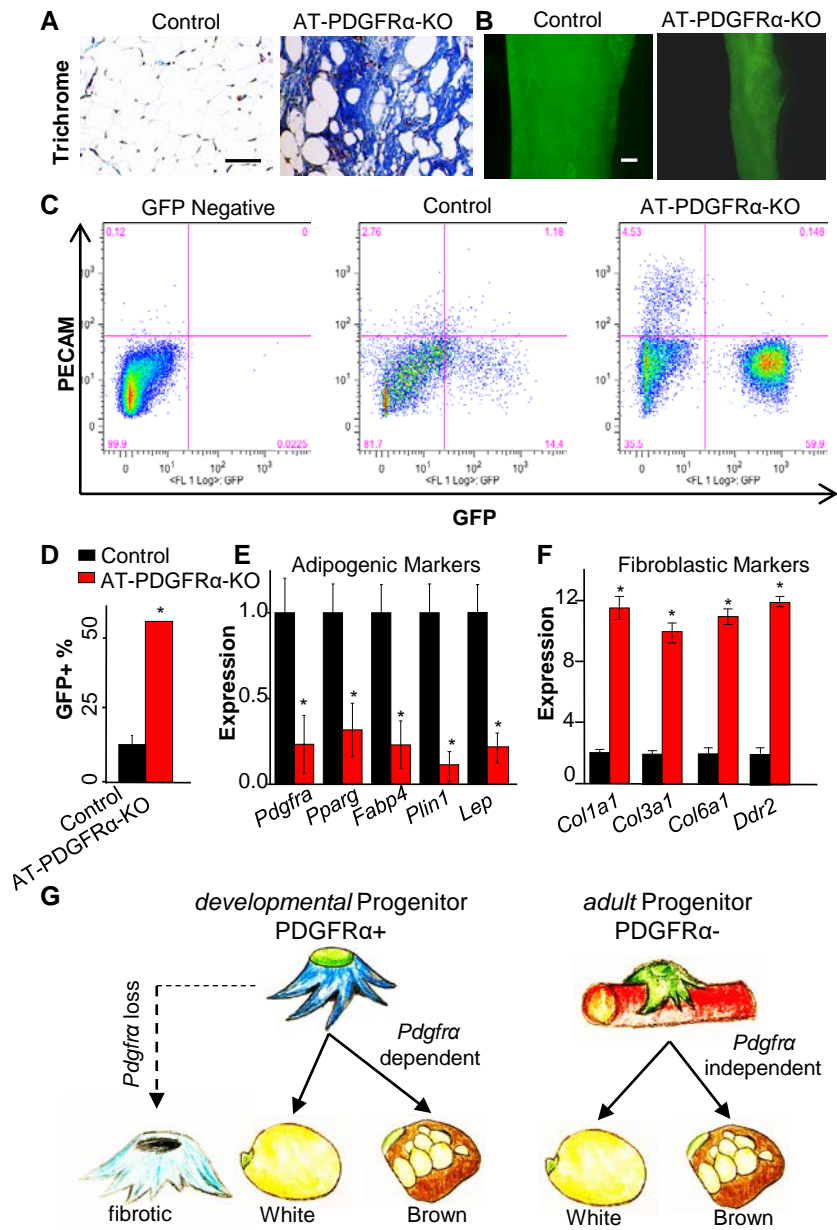


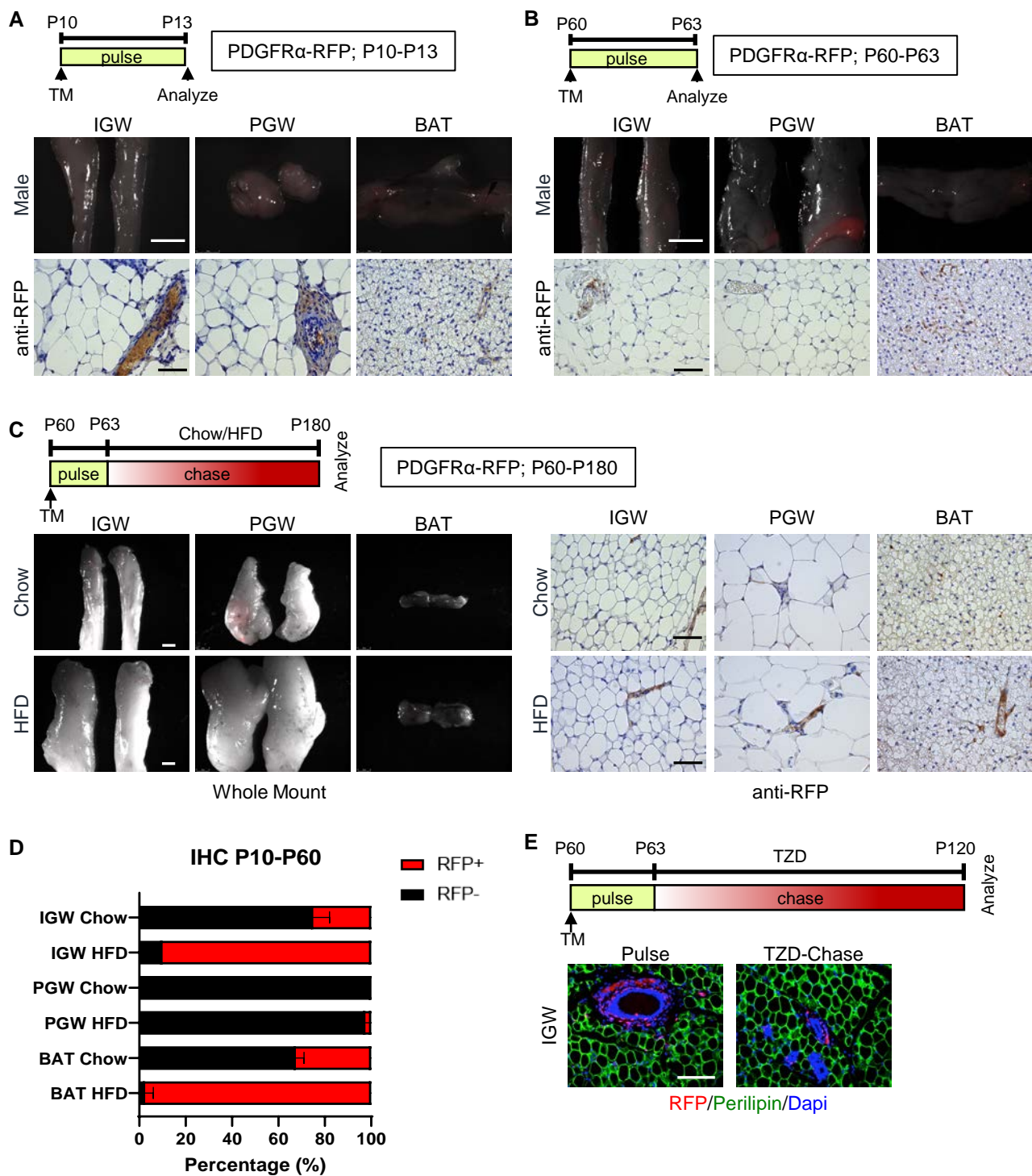


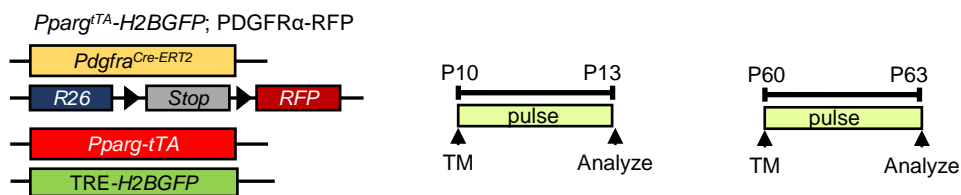
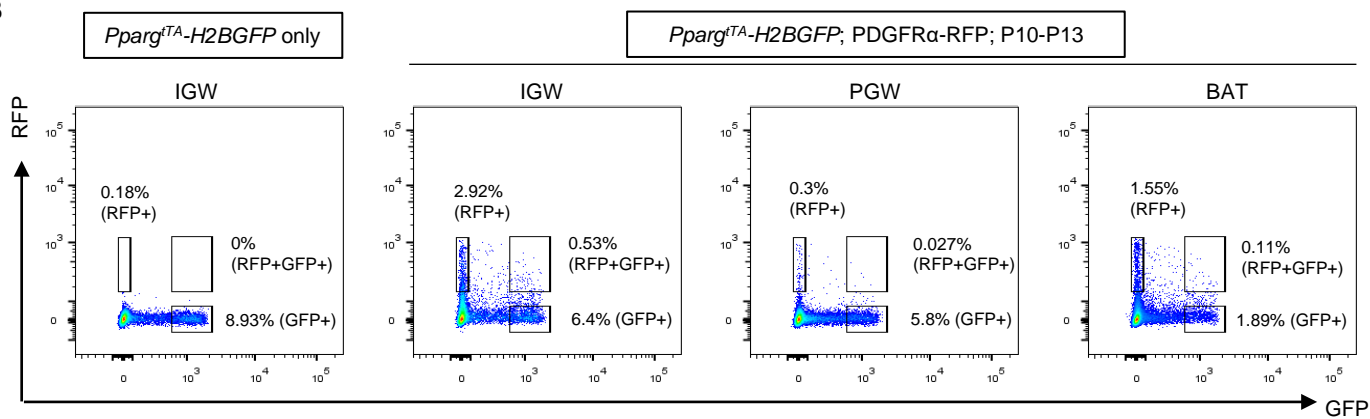










A**B****C**